DEVELOPMENT OF A VAPOR CLOUD EXPLOSION RISK ANALYSIS TOOL USING EXCEEDANCE METHODOLOGY

A Thesis

by

SALEM SAAD S. ALGHAMDI

Submitted to the Office of Graduate Studies of
Texas A&M University
in partial fulfillment of the requirements for the degree of

MASTER OF SCIENCE

August 2011

Major Subject: Safety Engineering

Development of a Vapor Cloud Explosion Risk Analysis Tool

Using Exceedance Methodology

DEVELOPMENT OF A VAPOR CLOUD EXPLOSION RISK ANALYSIS TOOL USING EXCEEDANCE METHODOLOGY

A Thesis

by

SALEM SAAD S. ALGHAMDI

Submitted to the Office of Graduate Studies of
Texas A&M University
in partial fulfillment of the requirements for the degree of

MASTER OF SCIENCE

Approved by:

Chair of Committee,	M. Sam Mannan
Committee Members,	Maria Barrufet
	Sergiy Butenko
Head of Department,	Michael Pishko

August 2011

Major Subject: Safety Engineering

ABSTRACT

Development of a Vapor Cloud Explosion Risk Analysis Tool

Using Exceedance Methodology.

(August 2011)

Salem Saad S. Alghamdi, B.S.; B.S., Colorado School of Mines

Chair of Advisory Committee: Dr. M. Sam Mannan

In development projects, designers should take into consideration the possibility of a vapor cloud explosion in the siting and design of a process plant from day one. The most important decisions pertinent to the location of different process areas, separation between different areas, location of occupied buildings and overall layout may be made at the conceptual stage of the project. During the detailed design engineering stage the final calculation of gas explosion loads is an important activity. However, decisions related to the layout and location of occupied buildings at this stage could be very costly. Therefore, at the conceptual phase of the development project for a hydrocarbon facility, it would be helpful to get a picture of possible vapor cloud explosion loads to be used in studying various options.

This thesis presents the analytical parameters that are used in vapor cloud explosion risk analysis. It proposes a model structure for the analysis of vapor cloud explosion risks to buildings based on exceedance methodology. This methodology was developed in a

computer program which is used to support this thesis. The proposed model considers all possible gas release scenarios through the use of the Monte Carlo simulation. The risk of vapor cloud explosions can be displayed using exceedance curves.

The resulting model provides a predictive tool for vapor cloud explosion problems at the early stages of development projects, particularly in siting occupied buildings in onshore hydrocarbon facilities. It can also be used as a quick analytical tool for investigating various aspects of vapor cloud explosions.

This model has been applied to a case study, a debutanizer process unit. The model was used to explore the different alternatives of locating a building near the facility. The results from the model were compared to the results of other existing software to determine the model validity. The results show that the model can effectively examine the risk of vapor cloud explosions.

DEDICATION

To my father and mother

To my wife and three sons

To my family

To my friends

ACKNOWLEDGEMENTS

I would like to thank my committee chair, Dr. Mannan, for his continuous support and inspiration to perform this research. I would like also to thank Dr. Maria Barrufet and Sergiy Butenko for serving on my committee. Special thanks to Dr. Hans Pasman for the support and help I received throughout my research.

Thanks also to my friends and colleagues and the department faculty and staff for making my time at Texas A&M University a great experience. I also want to extend gratitude to my wonderful company Saudi Aramco, which provided financial support for my study.

Finally, thanks to my mother and father for their encouragement and prayers and to my wife for her patience and love.

TABLE OF CONTENTS

CHAPTER Page

LIST OF FIGURES

FIGURE Page

LIST OF TABLES

CHAPTER I

INTRODUCTION

Research Motivation

On October 23, 1989, a vapor cloud explosion destroyed the facilities at the Phillips 66 Refinery in Pasadena, Texas. The explosion caused massive destruction to the control room and also severely damaged an administration building located 0.5 mi away. Twenty three fatalities and one hundred and thirty injuries resulted from the explosion. Property damage was estimated to be three-quarters of a billion dollars. The post-accident investigation revealed that 85,000 pounds of extremely flammable gas was released from an open valve during normal maintenance work on one of the polyethylene plant's reactors. As a result of the release, a vapor cloud formed and traveled quickly through the polyethylene plant. The vapor cloud ignited, within 90 to 120 seconds, and caused an explosion with the force of 2.4 tons of TNT [1].

On June 1st, 1974, the Nypro (UK) site at Flixborough was destroyed by a massive vapor cloud explosion resulting from a 20 inch bypass line rupture which led to the release of a huge amount of cyclohexane. Twenty eight fatalities and thirty six injuries resulted from the explosion.

This thesis follows the style of Process Safety Progress.

Had the explosion taken place on a weekday, the number of fatalities and injuries would have been higher. Out of the 28 fatalities, 18 took place in the control room because of the windows shattering and the roof collapse. None of those who were in the control room were able to escape [1].

The above two accidents are only two examples of incidents with a high number of fatalities inside occupied buildings. CCPS provides a list of other serious incidents involving buildings in process plants [2]. API RP752 estimates that the likelihood of a major explosion at any particular refinery is about 1 in 2,000 years [3]. There will always be a possibility of having an explosion when dealing with hydrocarbons. About 42% of largest losses in the hydrocarbon process industry were caused by vapor cloud explosions [4]. Lenoir and Davenport [5] have presented a review of many major incidents involving vapor cloud explosions worldwide from 1921 to 1991. Hydrocarbon materials such as ethane, ethylene, propane, and butane, which have been involved in the incidents indicated , have a greater potential for vapor cloud explosions. The impact of such explosions can be destructive, resulting in casualties and large financial losses. Often many of the serious injuries and fatalities take place inside occupied buildings on site. The design and location of occupied buildings on or around hazardous facilities has been a recurring topic as a result of these and similar accidents.

The explosion risk to people inside process plant buildings depends on the building construction type, location of the building, the plant processes and the materials. A

quantitative risk assessment can determine where risk is high and risk reduction measures, such as modifying the process, relocate the buildings, strengthen the building, or reduce occupancy in buildings, are suitable. The quantitative risk analysis, in essence, should predict the extent and movement of the gas cloud and calculate the overpressures generated if the cloud is ignited inside a congested area. This research is motivated by the industry's need to better improve the prediction of the consequences of vapor cloud explosion and to quantify the risks.

Background

In development projects, designers should take into consideration the possibility of a vapor cloud explosion in the siting and design of process plant from day one. Most important decisions pertinent to location of different process areas, separation between different areas, location of occupied buildings and overall layout may be made at the conceptual stage of the project. During the detailed design engineering stage the final estimation of vapor cloud explosion loads is one significant step. However, decisions related to the layout and location of occupied buildings at this stage could be very costly. Therefore, at the conceptual phase of the development project for a hydrocarbon facility, it would be helpful to get a picture of possible vapor cloud explosion loads to be used in studying various options. The amount of detailed information at this stage of the project is very little and, hence the use of complex explosion prediction models will be limited as they require the input of geometry details. Furthermore, conducting a detailed

explosion risk assessment at this stage of a project will not be reasonable due to the normal project schedule.

For these and other reasons, vapor cloud explosion risk analysis models are required to measure the potential explosive power of the flammable materials present in a process unit. To estimate overpressure which results from vapor cloud explosions is often part of a risk assessment. Risk assessment typically consists of five major elements (Figure 1); description and definition of the system, identification of hazards, frequency analysis, consequence analysis, and risk estimation [6]. The risk is the product of the likelihood of occurrence of a hazardous event and the consequences of that event. So in order to calculate the risk of explosions, it is essential to calculate the frequencies of events that would lead to a gas leak, and the overpressure that could result from such leak. The frequencies of leak and the potential overpressures should then be combined using an established methodology that takes into consideration the impact of atmospheric conditions and other related factors as well.

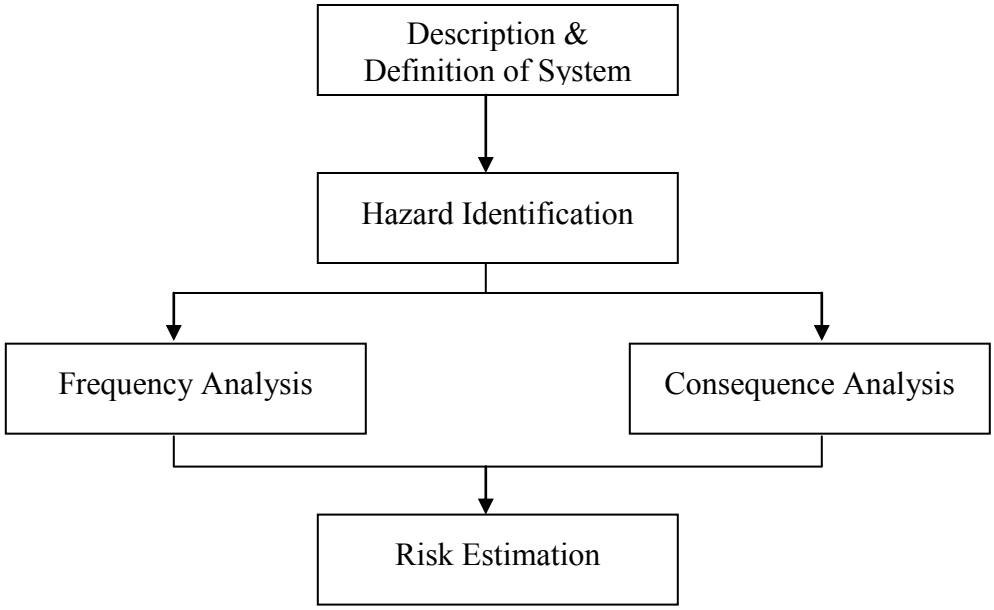

Figure 1. Flow chart of quantitative risk analysis.

Objectives of the Current Research

This thesis develops a quantitative risk assessment tool based on the exceedance methodology. The resulting tool has two main objectives:

- To provide a predictive tool for vapor cloud explosion problems at early stages of development projects, particularly in siting occupied buildings on onshore hydrocarbon facilities.

- To provide a quick analytical tool for investigating various aspects of the vapor cloud explosions.

Some of the current public domain risk assessment methodologies tend to rely on worst case explosions which are events of extremely low probability and may not represent the general population of explosion credible scenarios. In addition, full-scale gas explosion experiments revealed that design against such worst cases is impractical and expensive [7]. Thus, probabilistic approaches using complex Computational Fluid Dynamics (CFD) have become more common. However, probabilistic approaches result in thousands of scenarios due to variations of all input factors related to release size, weather data, and ignition which cannot be modeled using CFD except through categorization and extrapolation.

The aim of this thesis is to develop a methodology for the assessment of vapor cloud explosions associated with industrial settings of real world complexity. The proposed model will take into account all possible gas release scenarios through the use of Monte Carlo simulation. In addition, the risk of vapor cloud explosions will be displayed using exceedance analysis.

The methodology will be developed in a computer program where the above objectives can be directly explored.

CHAPTER II

SOURCE, DISPERSION AND IGNITION MODELS

Before a gas explosion is possible, there are several events that must occur, which involve a release of gas, a formation of gas cloud, and a delayed ignition. Calculating these events is considered vital when estimating the explosion overpressure. In this chapter, a comprehensive literature review of the available source, dispersion and ignition models will be presented. The selected models for the program have been explained in details.

Source Models

Source or release models [6,8] are used to calculate the quantity of material that has been released, or the rate of release. These models are considered vital in the process of risk analysis as the results of these models determine the size or the extent of the resulting cloud and consequently the probability of the ignition and explosion.

The initial discharge rate of a leak depends mostly on the chemical properties, pressure and temperature inside the process equipment, and the size of the crack or rupture. Hydrocarbon leaks are typically either in the form of gas, liquid, or two-phase. Examples of hydrocarbon gas releases are methane through butane, while liquid releases could be crude oil, diesel, jet fuel, or others. An example of a two-phase leak is condensate since it is a hydrocarbon mixture of mostly butane to hexane that condenses as a result of gas

compression. When this material is under high pressure, it is in the liquid phase but once the pressure is removed, it turns into gas. Identifying the correct phase and the proper model that goes with it is important in order to accurately estimate the risk. Source models for the liquid and gas-liquid releases are not considered in this research as the focus of the proposed program is on gaseous hydrocarbons such as ethane, propane and butane. The reason is that gas releases constituted the largest proportion of overall releases reported, i.e., 54% while other types of releases were oil (17.4%), non-process (11.6%), two-phase (8.0%) and condensate (7.3%) [9]. Details of the source model for gas releases from holes in process equipment, used in developing the program are explained in the following section.

Flow of a gas from a hole source model

Source models represent a significant part of the consequence modeling. Explosion accidents start with a release of flammable materials from the process equipment. Source models are used to determine the release rate, the total quantity released, and the state of the release (gas, liquid, or a combination). There are a number of source models and each is based on fundamental or empirical equations describing the physicochemical processes taking place throughout the release of materials. In any complex hydrocarbon plant, numerous source models are needed to explain the release.

The program assumes the flow of gases through holes as the source model. As the gas leaks and expands through the hole, the energy contained within the gas due to its

pressure is transformed into kinetic energy. The density, pressure, and temperature change as the gas discharges through the hole. Gas discharges in the program are assumed to be free expansion releases where the assumption of isentropic behavior is usually valid [8]. The mechanical energy balance in equation 1 describes the compressible flow of gases:

$$\int \frac{dP}{\rho} + \Delta\left(\frac{\bar{u}^2}{2\alpha g_c}\right) + \frac{g}{g_c}\Delta z + F = -\frac{W_s}{\dot{m}} \tag{1}$$

where

P is the pressure (force/area)

p is the density (mass/volume)

$\bar{u}$ is the average instantaneous fluid velocity (length/time)

g_c is the gravitational constant (length mass/force time^2)

α is the unitless velocity profile correction factor with the following values:

α = 0.5 for laminar flow, α = 1.0 for plug flow, and α→1.0 for turbulent flow,

g is the acceleration due to gravity (length/time^2)

z is the vertical height above datum (length)

F is the net frictional loss term (length force/mass)

W_s is the shaft work (force length)

$\dot{m}$ is the mass flow rate (mass/time)

Equation 2 is integrated along an isentropic path to determine the mass release rate. This equation assumes an ideal gas, no heat transfer and no external shaft work:

$$\dot{m} = C_0 A P_0 \sqrt{\frac{2g_c M}{R_g T_0}\frac{\gamma}{\gamma-1}\left[\left(\frac{P}{P_0}\right)^{2/\gamma} - \left(\frac{P}{P_0}\right)^{(\gamma+1)/\gamma}\right]} \qquad (2)$$

where

C_0 is the discharge coefficient (dimensionless)

A is the area of the hole (length^2)

P_0 is the pressure upstream of the hole (force/area)

M is the molecular weight of the gas (mass/mole)

γ is the heat capacity ratio, C_p/C_y (unitless)

R_g is the ideal gas constant (pressure-volume/mole-deg)

T_0 is the initial upstream temperature of the gas (deg)

P is the downstream pressure (force/area)

Equation 2 represents the mass flow rate at any point during the isentropic expansion. The majority of gas discharges from process plant leaks will initially be sonic or choked [10]. As the upstream pressure P_0 goes down (or downstream pressure P goes down), a maximum is found in equation 3. This maximum occurs when the velocity of the exiting gas achieves the sonic velocity. At this point, the flow becomes independent of the downstream pressure and is dependent only on the upstream pressure. The equation representing the sonic or choked case is:

$$\dot{m} = C_0 A P_0 \sqrt{\frac{\gamma g_c M}{R_g T_0}\left(\frac{2}{\gamma+1}\right)^{(\gamma+1)/(\gamma-1)}} \quad (3)$$

And the velocity can be also calculated using the following equation:

$$u = \sqrt{\frac{2 g_c R_g T_0}{M}\frac{\gamma}{\gamma-1}\left[1-\left(\frac{P}{P_0}\right)^{(\gamma-1)/\gamma}\right]} \quad (4)$$

For chocked flows, a conservative value of 1.0 for the discharge coefficient is recommended. Values for the heat capacity ratio γ for a variety of hydrocarbon gases are provided in Table 1.

Table 1. Heat capacity ratios and molecular weights for selected gases [8].

Gas	Molecular Weight (M)	Heat Capacity Ratio $\gamma=C_p/C_v$
Ethane	30.0	1.22
Propane	44.1	1.15
Butane	58.1	1.11

Gas Dispersion Models

The gas released due to an accidental leak or rupture is dispersed due to the initial momentum of discharge, turbulence caused by the surrounding obstacles, and the wind. Gas dispersion models are used to estimate the size of the cloud.

There are different types of releases on the onshore or offshore hydrocarbon facilities based on the degree of confinement and obstacles. These releases take place either in confined areas, in congested areas, in open areas, or under water. Modeling of gas dispersion in confined and congested areas requires the use of very sophisticated models such as computational fluid dynamic (CFD). However, CFD takes a lot of time to run and requires a lot of expertise. Alternatively, there are other gas dispersion models which model gas dispersion in open areas such as the box or SLAB models [1] for heavy gas dispersion and the Gaussian model [8] for neutrally buoyant dispersion. The proposed program is using the SLAB model due to its simplicity and because it is mainly intended for heavy gases such as Propane and Butane which are in line with the aim of the program.

SLAB model

The SLAB model was initially developed by Zeman [11] and its development has been further explained by Ermak, Chan, et al. [12]. It is mainly intended for a continuous release. The model is comprised of six differential equations for the conservation of

mass, material, momentum, and energy. It is a one-dimensional model with cloud properties averaged in the vertical and horizontal directions.

The basic conservation equations used by SLAB are presented below. These are the equations used in the steady state plume mode in which the independent variable is the downwind distance, x. The equations used by SLAB are:

Species

$$\frac{d(pUBhm)}{dx} = p_s W_s B_s \tag{5}$$

Mass

$$\frac{d(pUBh)}{dx} = p_a (V_e h + W_e) + p_s W_s B_s \tag{6}$$

Energy

$$\frac{d(pUBhC_pT)}{dx} = p_a (V_e h + W_e B) C_{pa} T_a + p_s W_s B_s C_{ps} T_s + f_t \tag{7}$$

X-Momentum

$$\frac{d(pUBhU)}{dx} = -0.5 \propto_g g \frac{d[(p-p_a)h^2 B]}{dx} + p_a (V_e h + W_e B) U_a + f_u \tag{8}$$

Y-Momentum

$$\frac{d(pUBhV_g)}{dx} = g(p - p_a)h^2 + f_{vg} \quad (9)$$

Cloud half-width

$$U\frac{dB}{dx} = (p_a/p)V_e + V_g \quad (10)$$

$$U\frac{db}{dx} = V_g \cdot b/B \quad (11)$$

Cloud height parameter

$$U\frac{dZ_c}{dx} = W_c \quad (12)$$

Equation of state

$$pT = \frac{p_a T_a M_s}{[M_s + (M_a - M_s)m]} \quad (13)$$

where

x = downwind distance, m

U = velocity in the direction of the wind, m/s

ρ = density, kg/m3

h = cloud height parameter, m

B = cloud width parameter, m

m = mass fraction of source gas

T = temperature, K

g = gravity constant, m/s^2

Cp = specific heat, J/(kg K)

fu = downwind friction term, kg/s^2

ft = ground heat flux, J/(m s)

fv = crosswind friction term, kg/s^2

Vg = horizontal crosswind gravity flow velocity, m/s

Ve = horizontal entrainment rate, m/s

We = vertical entrainment rate, m/s

M = molecular weight, kg/kmole

Ws = vertical source gas injection velocity, m/s

Ue* = friction velocity, m/s

a = refers to ambient properties

s = refers to source properties

The horizontal and vertical entrainment rate, Ve and We, are calculated using the following equations:

$$W_e = \frac{\sqrt{3}akU_{e*}g(1-h/H)}{\emptyset(h/L)} \quad (14)$$

$$V_e = \sqrt{3}(V_a^2 + V_j^2)^{1/2} \quad (15)$$

where

k = constant, 0.41

a = constant, 1.5

U_{e*} = friction velocity, m/s

L = Monin-Obukhov length derived from the atmospheric stability class

The Monin-Obukhov function, , $\emptyset(h/L)$ is defined by:

$$\emptyset(h/L) = \begin{cases} 1 + 5\frac{h}{L} & L \geq 0 \text{ (stable)} \\ \left[1 - 16\frac{h}{L}\right]^{-1/2} & L < 0 \text{ (stable)} \end{cases} \quad (16)$$

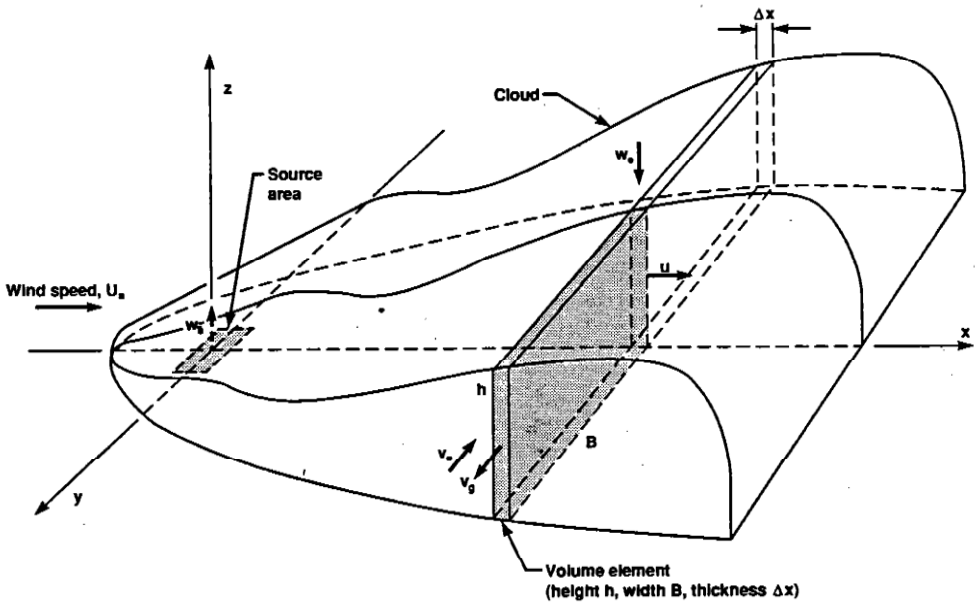

Figure 2. Schematic of heavy gas plume as depicted by SLAB model [13].

The variables are illustrated in Figure 2. In order to solve the above equations, a new variable must be defined and the conservation equations should be rearranged. The twelve equations (5-16) represent the basic equations for a steady state plume. A new variable, $R=\rho UBh$, is defined since it is common to the first five equations 5-9. When R is substituted into equation 6, it becomes dR/dx, which then can be integrated using the forth-order Runge-Kutta numerical method [14]. Runge-Kutta is also used to integrate all the other conservation equations. When R is calculated, equation 5 then is integrated, and an expression for the average cloud mass concentration is determined. Once the net ground heat flux is defined in equation 7, the equation can be solved by substituting in equations 5 and 6 and integrating to give an equation for the average cloud temperature. Equation 13 is solved to obtain the density, p. Substituting equations 5 and 6 into equation 8 and integrating, results in a cubic equation for velocity. The average wind speed can be used instead of the ambient wind speed term and then Simpson's rule is used to integrate the new equation. The source area can be increased until a solution is found. In order to solve equation 9, a gravity flow equation ($G=RV_g$) is defined and it's derivative is set equal to the right hand side of equation 9. The new equation is then integrated using the Runge-Kutta numerical method. The other three equations (10,11 and 12) are solved using the Runge-Kutta method, and the cloud height, h, can be determined by rearranging the equation for the new variable (R) which was defined initially to solve the equations.

Ignition Models

Different models exist to estimate the probability of ignition some of which are based on the size of the gas cloud [15,16], while others are more complex and include factors [17,18] such as the number and density of ignition sources, type of facility, time-dependent ignition, etc. The model which was developed by Cox, et al. [19] has been employed by the present research.

Cox ignition model

The program calculates the probability of ignition based on a correlation suggested by Cox, et al [19]. The correlation assumes that the probability of ignition is proportional to the power of the mass flow rate for continuous gas releases. Based on historical and observed data, the probability of ignition is approximately given by [20]:

$$P = 0.017\ m^{0.74} \tag{17}$$

where m denotes the mass flow rate. The correlation was derived based on the assumption that for a massive leak of 50 kg/s, the probability of ignition is 0.3 based on historic ignition probability for blowouts given by Dahl et al [21], and that for a minor leak of 0.5 kg/s, the probability of ignition given by Kletz [22] is 0.01. The program sets the highest value of ignition probability to equal the historic ignition probability for blowouts which is 0.3 [23].

CHAPTER III

VAPOR CLOUD EXPLOSION CONSEQUENCE MODELING

An overview of vapor cloud explosion consequence modeling is presented in this chapter. A literature review of vapor cloud explosions and all types of models that have been used for analyzing the overpressure from vapor cloud explosions is discussed in the following sections.

Vapor Cloud Explosion

A vapor cloud explosion is a process where a combustion of a premixed gas results in a rapid increase in pressure. Before a vapor cloud explosion is possible, there are several events that must occur. These events are illustrated in Figure 3. As the figure shows, it is essential to have a release of gas in order to have an explosion. Secondly, ignition must be present to ignite the released gas, which could result in fire or an explosion [24].

Vapor cloud explosions can take place in buildings or offshore modules, inside process equipment or pipes, in open process areas, or in unconfined areas. The vapor cloud explosions are classified based on the environment in which the explosion occurs. There are generally three types of explosions [24]:

- Confined gas explosions within vessels, pipes, channels or tunnels
- Partly confined gas explosions in compartments, buildings or offshore modules.

- Unconfined gas explosions in process plants and other unconfined areas.

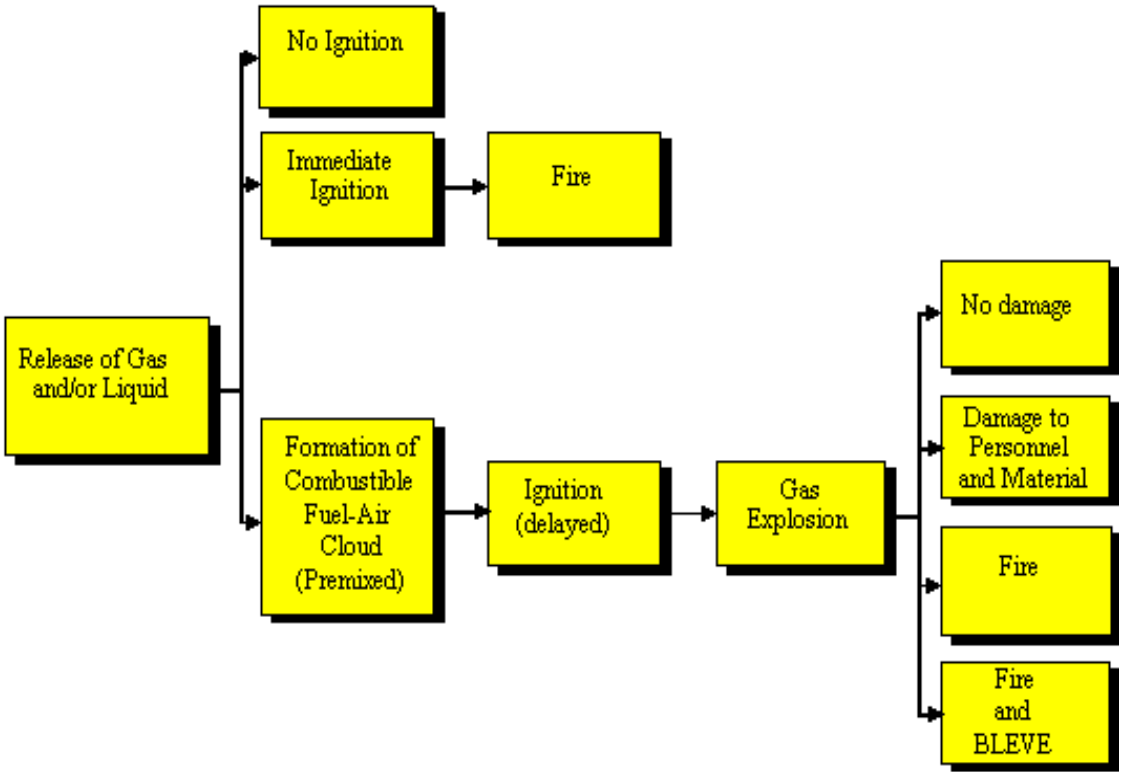

Figure 3. Events leading to gas explosion. BLEVE – Boiling Liquid Expanding Vapor Explosions [24].

An unconfined vapor cloud explosion in a processing plant can involve partly confined explosions in closed modules or highly congested areas where the vapor cloud has leaked. Confined vapor cloud explosions, so called internal explosions, are explosions which take place within processing equipment, tanks, pipes, sewage systems, culverts, and closed rooms. The combustion process in this kind of explosion does not need to be quick to result in a severe pressure increase. Partly confined explosions take place when

flammable material is accidentally discharged inside a building which is partly open, such as compressor rooms and offshore modules. The building will contain the explosion but the explosion overpressure can only be relieved through the explosion vent panels, or through breakdown of the surrounding walls [24].

Unconfined vapor cloud explosions take place in open areas such as hydrocarbon and petrochemical processing plants. It has been demonstrated in large-scale tests that an actually unconfined, unobstructed flammable vapor cloud ignited by a weak ignition source will lead to flash fire. In a real hydrocarbon processing plant, however, there are partly confined and obstructed local areas such as pipe racks which could cause deflagration with high overpressures. A deflagration has a limited burning velocity, in the range 100–500 m/s. On the other hand, if an unconfined vapor cloud detonates, the resulting overpressure will be very high, in the order of 20 bars. Most vapor cloud explosions on onshore and offshore hydrocarbon processing plants would fall into the category of deflagrations [24]. The focus of the present research is on unconfined or partially confined vapor cloud explosions.

Vapor Cloud Explosion Modeling

When examining the vapor cloud explosion overpressure prediction methodologies, it was found that there exist different models which vary from simple empirical models to more sophisticated and complex models. These models have been classified as follows:

- Empirical models: These models are based on correlations developed from analysis of experimental data. They are considered very simple models and their applicability is very limited. In addition, these models cannot handle complex geometries and as a result, they have significantly simplified the physics. Despite all aforementioned limitations, these models can be usefully used for quick order-of-magnitude calculations and for screening purposes for more analysis with more complex models. Examples of empirical models are TNT model [1], TNO multi-energy model [25], Baker Strehlow model [26], Congestion Assessment Method (CAM) [27,28].

- Phenomenological models: These models are slightly more complex and have a broader range of applicability than the previous models. These models are based on differential and algebraic equations which describe the physical process involved in the vapor cloud explosions. These models can model certain types of geometry by representation of an idealized system. In terms of sophistication, phenomenological models are somewhere between empirical models and complex Computational Fluid Dynamics models. These type of models has short running times and can run a large number of different scenarios. Examples of phenomenological models include SCOPE (Shell Code for Overpressure Prediction in gas Explosions) [29], CLICHE (Confined LInked CHamber Explosion) [30].

- Computational Fluid Dynamic (CFD) models: CFD models find the numerical solutions of the Navier-Stokes equations which govern the fluid flow. The numerical solutions are developed by discretizing the solution domain in both space and time. CFD has a wide range of applicability and can be used in many different disciplines. When comparing CFD with empirical and phenomenological models, CFD provides greater flexibility and accuracy. However, the main limitations of CFD are the process run time and the complexity of using it. Examples of available CFD models include CFX, AutoREAGAS, EXISM, and FLACS [31].

After analyzing the above three categories, empirical models were found to be suitable for the present research due to their simplicity, short run times, and suitability for being embedded in a risk assessment program. Existing empirical models have been tested and validated for modeling vapor cloud explosions in partially confined and highly congested conditions. Fitzgerald [32] presented an assessment of all empirical models, comparing them with the experimental data. It was suggested that the Congestion Assessment Method [28] is more appropriate in case of assessing a worst-case scenario whereas TNO multi-energy model [25] in cases of predicting the average overpressure for different explosion scenarios. The later was selected for the risk assessment tool in the current research.

TNO multi-energy model

The TNO multi-energy method [25] assumes that a strong blast is only generated in places with a large degree of congestion, while other parts of the cloud which are not confined or obstructed just burn out without any considerable contribution. It also assumes hemispherical gas clouds at stoichiometric concentrations with a constant flame velocity. In addition, the method can calculate the static and dynamic overpressure as well as the phase duration of several consecutive explosions in congested regions separated by unobstructed volumes. However, for the purposes of the present research, a restriction was made to the single explosion and the static overpressure.

The following steps outline the multi-energy concept for the vapor cloud explosion blast model [33]:

- When the volume of the gas cloud in the confined region is determined from the dispersion model, the energy released can be calculated from:

$$E = V*H_c*eff \tag{18}$$

where

E = energy released (MJ)

V = volume of the gas cloud in the confinement (m^3)

Hc = Heat of combustion (3.5×10^6 J/m^3 which is the heat of combustion of an average stoichiometric hydrocarbon-air mixture)

eff = efficiency of the explosion (0.15 - 0.4)

- The strength of the blast should be estimated. A more conservative assessment of strong blast strength can be estimated if a maximum strength of 10 is used. However, a blast strength of 7 appears to further accurately characterize real experience. The current version of the proposed program always assumes a blast strength of 7.

- Using the energy released, *E,* at some distance, *R,* from a blast source, the Sachs scaled distance is calculated by the following equation:

$$\bar{R} = \frac{R}{\left(E/P_0\right)^{1/3}} \tag{19}$$

where

$\bar{R}$ = Sachs-scale distance from charge (-)

R = real distance from charge (m)

E = charge combustion energy (J)

P_0 = ambient pressure (Pa)

- The blast charts in Figures 4 and 5 can be used to determine the Sachs-scaled blast side-on overpressure and positive-phase duration using the estimated blast strength and the Sachs scaled distance calculated above. After that, the real blast

side-on overpressure and positive-phase duration can be calculated using the following two equations:

$$P_s = \Delta\bar{P}_s \times P_o \tag{20}$$

and

$$t_+ = \bar{t_+}\left[\frac{\left(E/P_0\right)^{1/3}}{c_0}\right] \tag{21}$$

where

P_S = side-on blast overpressure (Pa)

ΔP_S = Sachs-scaled side-on blast overpressure (-)

P_0 = ambient pressure (Pa)

$t+$ = positive-phase duration (s)

$t+$ = Sachs-scaled positive-phase duration (-)

E = charge combustion energy (J)

C0 = ambient speed of sound (m/s)

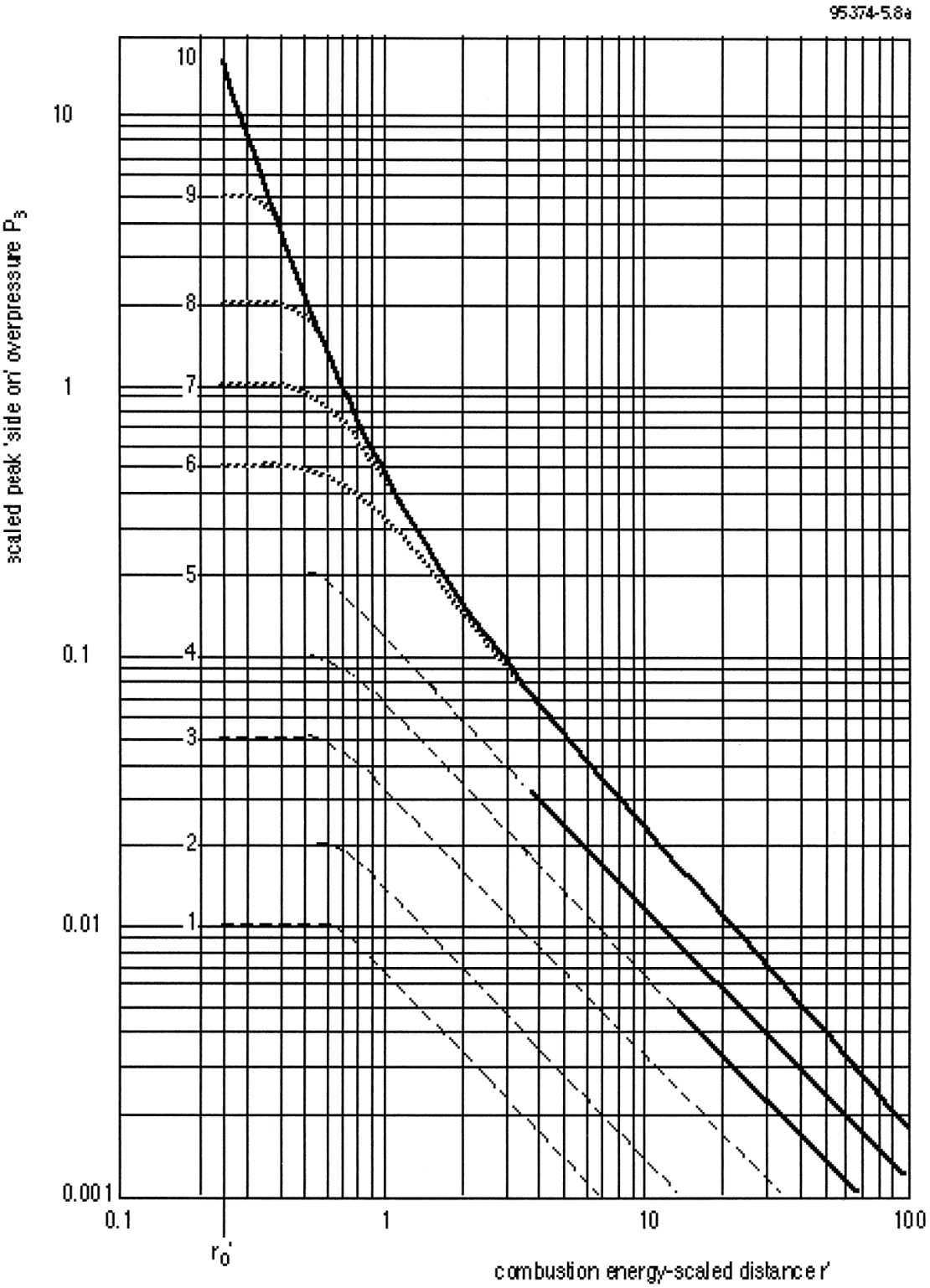

Figure 4. Chart for blast overpressure according to the multi-energy method [33].

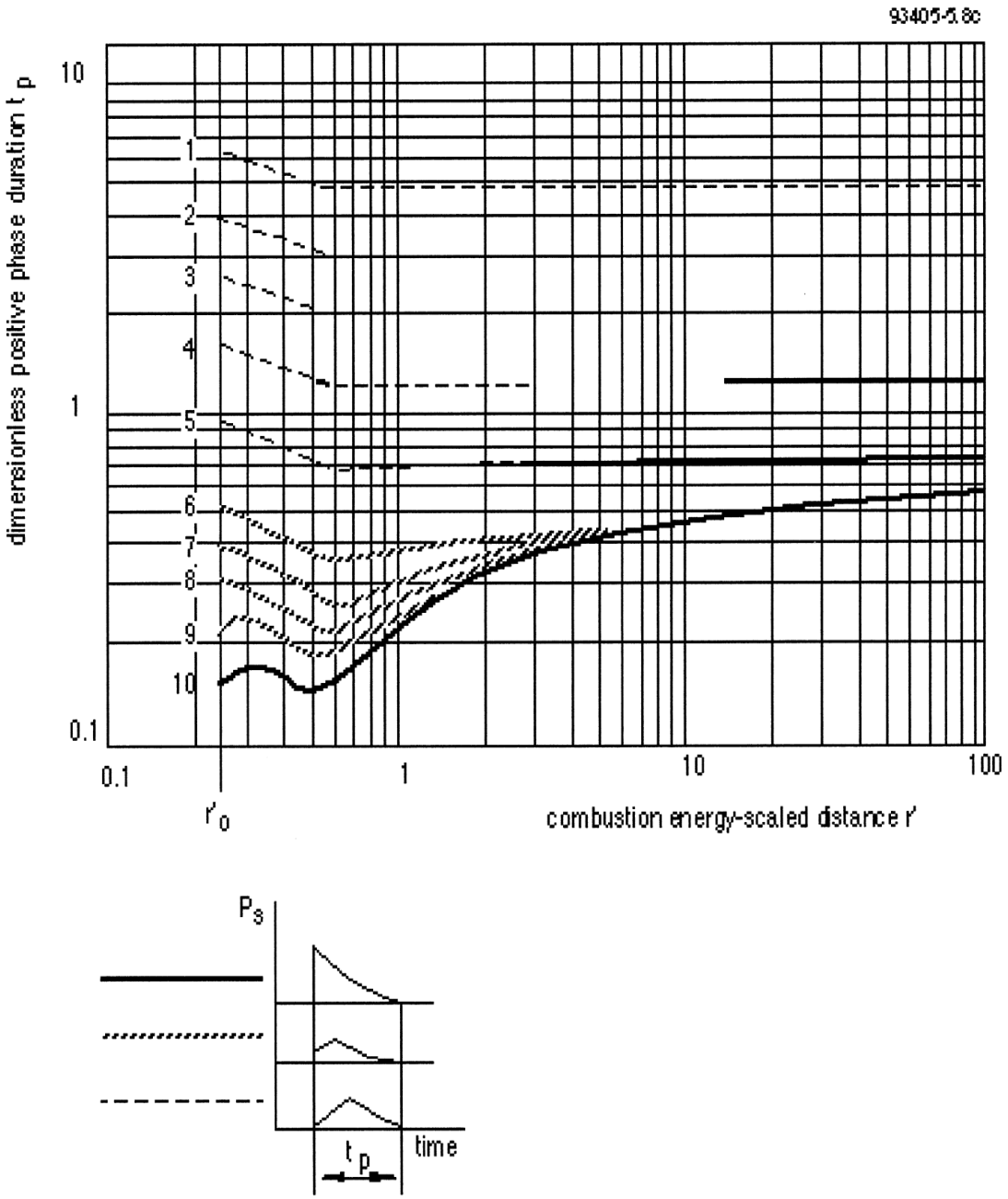

Figure 5. Chart for blast duration according to the multi-energy method [33].

Explosion Damage Effects

It is obvious that the damage caused by the explosion is a function of the overpressure, the form of the blast wave. In order to understand how the pressure is measured as the blast wave passes, imagine a pressure transducer is at a right angle to the blast wave, then the measured overpressure is the side-on overpressure. The side-on overpressure increases rapidly to its peak value, hence it is called peak side-on overpressure, and then decreases as the blast wave passes. To indicate what the blast damage of an explosion could be, Table 2 shows the damaging effects as a function of peak overpressure. The table illustrates that considerable damage is expected at even the small overpressures. In general, the damage is also a function of the rate of pressure increase and the duration of the blast wave. Therefore, the use of peak overpressure as a damage indicator is only very approximate. It is the time/pressure profile, i.e. impulse, of the blast wave combined with the structural response to that loading which determines the amount of damage.

Table 2. Damage estimates produced by a blast wave [34].

Peak side-on overpressure		Damage
(psi)	(kPa)	
0.02	0.14	Annoying noise (137 dB), if of low frequency (1–15Hz)
0.03	0.21	Occasional breaking of large glass windows already under strain
0.04	0.28	Loud noise (143 dB); sonic boom glass failure
0.1	0.69	Breakage of windows, small, under strain
0.15	1.03	Typical pressure for glass failure
0.3	2.07	"Safe distance" (probability 0.95 no serious damage beyond this value)
		Missile limit; Some damage to house ceiling; 10% window glass broken
0.4	2.76	Limited minor structural damage
0.5–1.0	3.5–6.9	Large and small windows usually shattered; occasional damage to window frames
0.7	4.8	Minor damage to house structures
1.0	6.9	Partial demolition of houses, made uninhabitable
1–2	6.9–13.8	Corrugated asbestos shattered, Corrugated steel or aluminum panels, fastenings fail, followed by buckling, Wood panels, fastening fail, panels blown in
1.3	9.0	Steel frame of clad building slightly distorted
2	13.8	Partial collapse of walls and roofs of houses
2–3	13.8–20.7	Concrete or cinder block walls, not reinforced, shattered
2.3	15.8	Lower limit of serious structural damage
2.5	17.2	50% destruction of brickwork of houses
3	20.7	Heavy machines (3000 lb) in industrial building suffer little damage
		Steel frame building distorted and pulled away from foundations
3–4	20.7–27.6	Frameless, self-framing steel panel building demolished
4	27.6	Cladding of light industrial buildings ruptured
5	34.5	Wooden utilities poles (telegraph, etc.) snapped Tall hydraulic press (40,000 lb)
5–7	34.5–482	Nearly complete destruction of houses
7	48.2	Loaded train wagons overturned
7–8	48.3–55.1	Brick panels, 8–12 in. thick, not reinforced, fail by shearing or flexure
9	62.0	Loaded train boxcars completely demolished
10	68.9	Probable total destruction of buildings; Heavy (7000 lb) machine tools moved and badly damaged, Very heavy (12,000 lb) machine tools survived
300	2000	Limit of crater lip

CHAPTER IV

VAPOR CLOUD EXPLOSION MODEL DEVELOPMENT

This chapter describes the details of the quantitative risk calculations included in the developed program. All the procedures explained in the chapter are implemented in the program.

Introduction

The Vapor Cloud Explosion (VCE) program is a system which models the explosion risk of an accidental release of a hydrocarbon gas. Its aim is to assist designers to produce safe and cost effective modifications to existing or new site layouts, particularly in-plant buildings sitings and designs. Alternatively, it may provide a screening tool for explosion overpressure calculations in quantitative risk assessment studies at the conceptual phase of a project.

The accidental release and ignition of flammable gas in hydrocarbon facilities presents potential explosion hazards that can impact the safety of plant personnel and plant assets. This research provides a computer program to determine the explosion risk to occupied buildings on the site. The methodology employed in the program calculates the frequency and distribution of potential explosion overpressures from a user-defined process module. The results are expressed as a plot of probability of exceeding a given overpressure against that overpressure.

In reality there are several situations under which flammable gas may be released and ignited, resulting in different consequences. All the following factors may vary [35]:

- Leak location
- Composition of material released
- Phase of material released (gas, liquid, two-phase)
- Leak size, leak rate and leak orientation
- Atmospheric stability, wind speed and direction
- Ignition location
- Time of ignition

Each factor above has a frequency or probability distribution associated with it. They all affect the magnitude as well as the frequency of the overpressure generated by vapor cloud explosions. The result can be shown as a plot of probability of exceeding a given overpressure against that overpressure.

For simplicity, the computer program that was developed and is presented in this research focuses on variations pertaining only to leak location, hole size, atmospheric stability, and wind speed and directions. The other factors are assumed to be fixed. In addition, the congestion inside the module which affects the overpressure generated by the explosion is taken into account as part of the multi-energy explosion model.

Methodology Overview

Figure 6 illustrates the steps for generating an overpressure exceedance curve. The proposed methodology starts with a description of the module including the number of pieces of equipment and the number of virtual leak locations. In addition, all information needed to define the leak scenario such as the type of fuel, operating pressure and temperature, and hole size is necessary to calculate the release rate using the flow of gas through a hole source model. The selection of the hole size, leak location, wind speed, wind direction and stability class in the program are done randomly using the Monte Carlo simulation. Then, a dispersion model (SLAB) estimates the volume of the gas cloud using the release rate and location as well as weather conditions. The calculated cloud volume and the calculated distance from the center of the cloud to the building are fed into the multi-energy explosion model to calculate the side-on overpressure. At the same time, the frequency of each scenario is calculated using the calculated frequency of leak in the module and the probabilities of leak size, leak location, weather conditions, and ignition. This process is repeated thousands of times based on the number of iterations defined by the user. In each iteration, a side-on overpressure and frequency is calculated and stored. Once all iterations are completed, the stored overpressures and frequencies are used to generate the exceedance curve.

The methodology has been programmed using Visual C++ from Microsoft Visual Studio 2010. The program has been designed to calculate the overpressure exceedance curves to assist with quantitative risk assessment studies of hydrocarbon process facilities based

on the information input by user of the release properties, process module and weather variations.

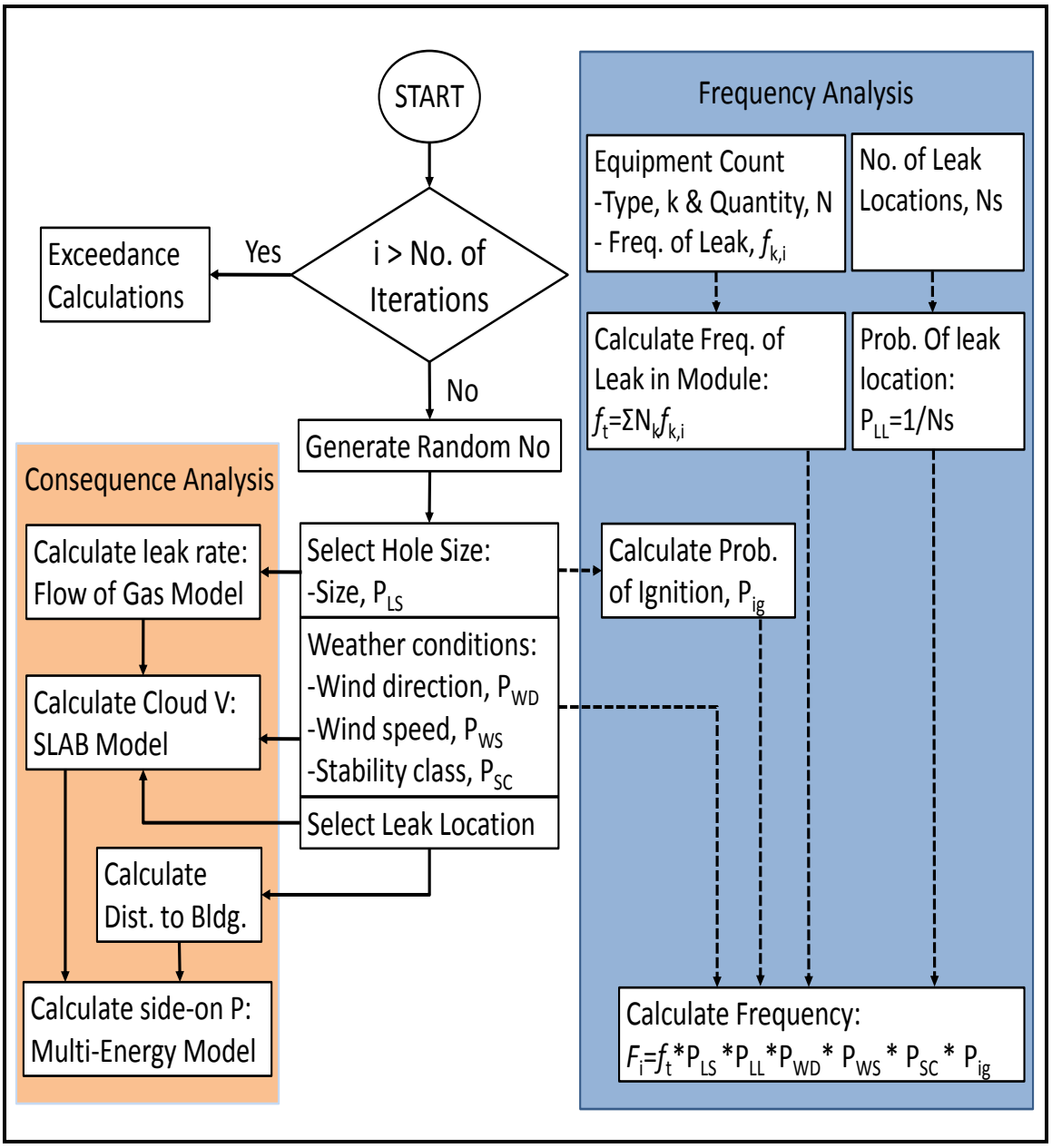

Figure 6. The overall methodology of the program.

User-Defined Information

The sequence of operation by the proposed program is shown in Figure 7. Details of the these operations are explained in details in the subsequent sections.

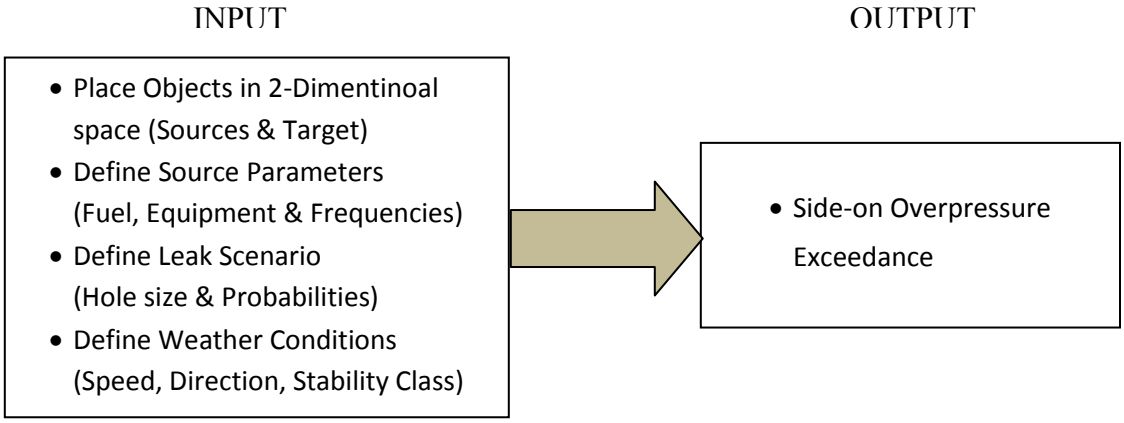

Figure 7. Sequence of operations by the developed program.

The module concept

A typical process site contains a large number and variety of process equipment, which needs to be modeled at an appropriate level of detail. Because of the multitude of process equipment, often several storeies high, it is not feasible to display all process equipment on the screen and model them individually. A method of aggregation is developed to simplify the risk modeling without affecting the accuracy.

The module combines a number of different types of equipment into a single object. Any plant can thus be built up by a set of modules, which represent their true physical extent. Each module represents an interconnected section of the process, with a given type of

fluid and with the process pressure and process temperature in the same range/order of magnitude. The user specifies the pressure and temperature for the releases. Using a conservative approach, the inventory or throughput in a process module is assumed to be infinite.

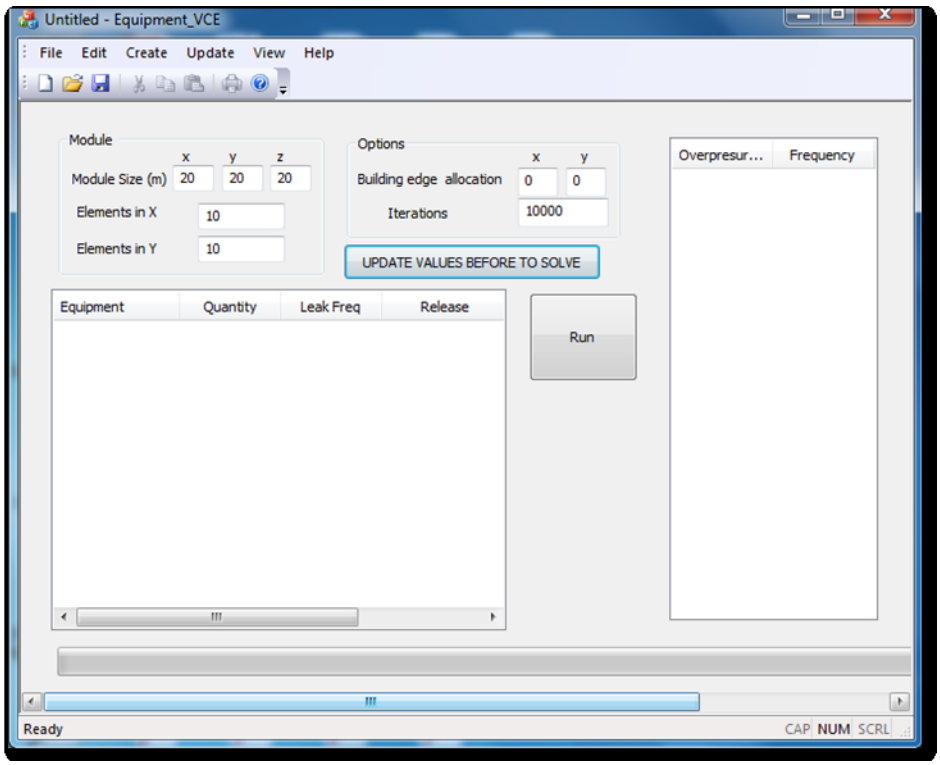

Figure 8. The main window of the program.

The program uses 2-dimentinal space system to locate the module, buildings, leak points and so on. In the main window of the program shown in Figure 8, the user can define the size of the process module by defining the length of each dimension in the x, y and z directions. The dimensions are entered in meters. The program always assumes the (0,0) point as the center of the module.

In the same window, the user can also define the location of the edge of the building by defining the x and y coordinates with respect to the center of the module, as shown in Figure 9. The distance is then can be calculated from any point in the module to the edge of the building.

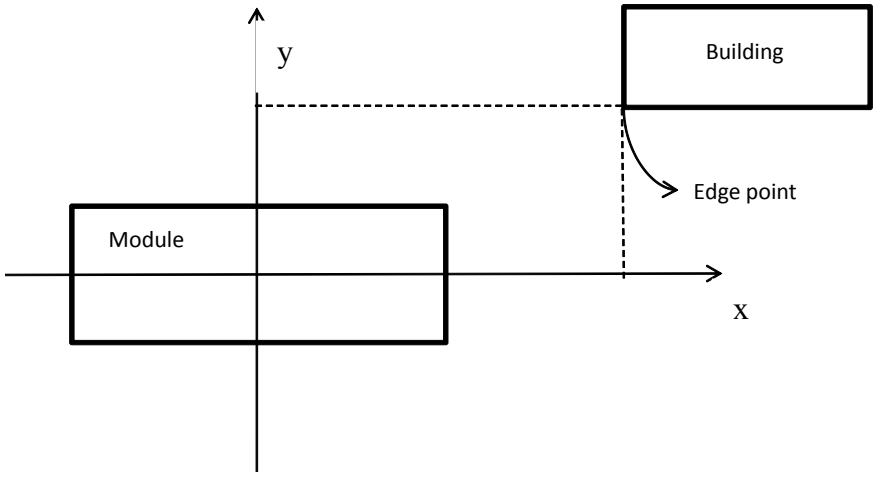

Figure 9. Schematic showing an example of the location of a module and a building.

Equipment count

The next step of the methodology is to enter the number of equipment in the defined module and the associated leak frequencies. This step is important to calculate the leak frequency in the module which will be used in the frequency analysis described later in subsequent sections. The types of equipment available to the user are:

- Process Vessels
- Pumps (Centrifugal & Reciprocating)

- Compressors ((Centrifugal & Reciprocating)
- Heat Exchangers
- Pipelines
- Flanges
- Valves
- Fittings

The user can select the types of equipment that exist in the module from the drop-down list as shown in the equipment count dialog box in Figure 10. After that, the user can enter the name and the number of the selected type as well as the leak frequency. In the case of pipelines, the user can define the length in meters as the quantity.

Once the user selects the type of equipment, a default generic leak frequency associated with that type of equipment is displayed. The user can change the default generic leak frequency if he wishes to. The equipment leak frequencies stored in the program are based on the E&P Forum database [23].

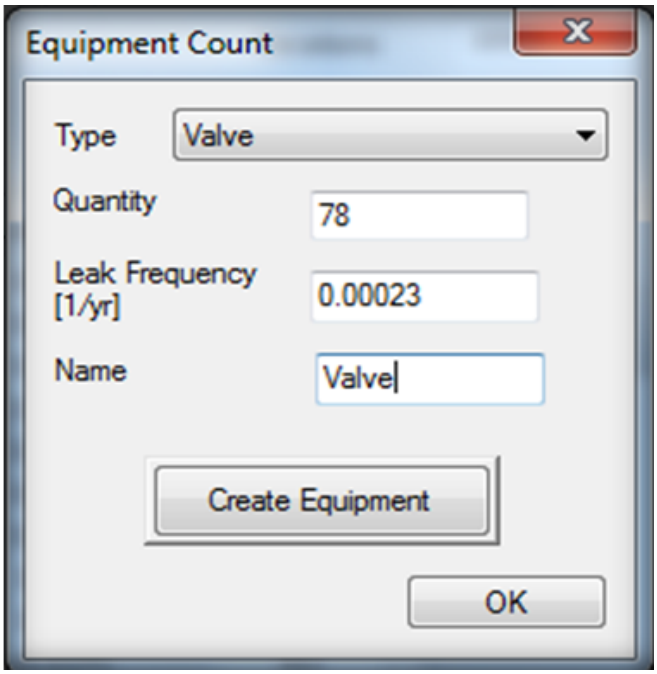

Figure 10. Equipment count and leak frequencies dialog box.

Multiplying the module's equipment count by a generic leak frequencies simply approximate the likelihood of leaks which gives an indication of the size and complexity of the module. This can be combined with the leak consequences to calculate the overall risk. The dominant leak sources can then be identified and proper management measures implemented [36].

Release scenarios

This section describes the user-defined information for the release scenarios. The characteristics of the release or leak, such as the fuel type, operating conditions or size of the leak, is crucial to estimate the release rate and hence, the extent of the gas cloud. Each process module comprises of different types of leaks such as flanges leak,

connections leak, fittings leak, pipelines leak, seal leak, catastrophic or rupture leak and general leak. Each leak is spread equally over the process module area. The leak types, defined using the process module concept, are identical, with each leak sharing the same fuel, flammable, and process conditions. Thus, the main distinguishing feature between release scenarios is the hole size specified.

The dialog box shown in Figure 11 is used to specify each of the leak hole sizes. The leak probability for each of the hole sizes is specified as a percentage split of the effective leak frequency calculated for the leak. The leak probabilities of the hole sizes are then used by the program to generate the cumulative probability distribution which is used by the Monte Carlo to randomly select the hole size. Numerous resources that contain data on hole size distribution are available in the literature [23, 36, 37].

In addition to specifying the hole size, the user can define the fuel type, the source pressure and source temperature. The present version of the program comprises of three hydrocarbon fuels, which are ethane, propane, and butane. Using a conservative approach, the user can use the worst operating conditions (pressure and temperature) in the process module for the calculations.

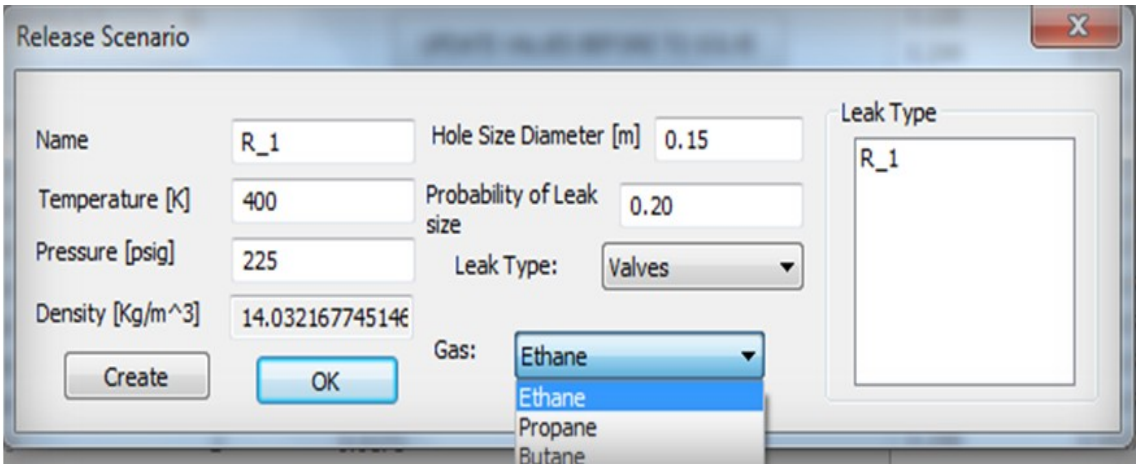

Figure 11. Dialog box for defining the release characteristics.

Weather variations

The weather is divided into a number of so-called Pasquill weather classes which depend on the ambient temperature. The Pasquill weather classes used are typically characterized as shown in Table 3.

Table 3. The Pasquill stability classes [8].

Stability class	Definition	Stability class	Definition
A	Extremely unstable conditions	D	Neutral conditions
B	Moderately unstable conditions	E	Slightly stable conditions
C	Slightly unstable conditions	F	Moderately stable conditions

These weather types influence the dispersion distances of gas clouds; in principle the quieter the weather type, the further a cloud may go. The dispersion distance is also

influenced by the wind speed. Table 4 shows the weather conditions that define the stability class.

Table 4. Meteorological conditions that define the Pasquill stability classes [8].

Surface Wind Speed		**Daytime Incoming Solar Radiation**			**Nighttime Cloud Cover**	
m/s	mi/h	Strong	Moderate	Slight	> 50%	< 50%
< 2	< 5	A	A – B	B	E	F
2 – 3	5 – 7	A – B	B	C	E	F
3 – 5	7 – 11	B	B – C	C	D	E
5 – 6	11 – 13	C	C – D	D	D	D
> 6	> 13	C	D	D	D	D

The weather conditions dialog box shown in Figure 12 enables the user to specify the wind rose data used for dispersion calculations. First, the Pasquill stability class is selected by the user through the drop down list. In order to enter the probability of the stability class the user should highlight the stability class and then input the probability. After that, the user may select the wind speed and its associated probability. The user can define as many wind speeds as necessary. The user can associate a stability class with a wind speed by highlighting the stability class and then selecting a wind speed (i.e. D5 or F2). The user needs to click on the arrows >> to enter the values.

The wind direction is defined as being in a given sector (blowing to rather than from a sector). Normal meteorological convention gives the angle as the direction the wind is blowing from. For example, a northerly wind blows from the north to the south, in

program terms this would be a 180^{o} wind. Zero degrees is to the North and wind angles are specified in a clockwise direction from North.

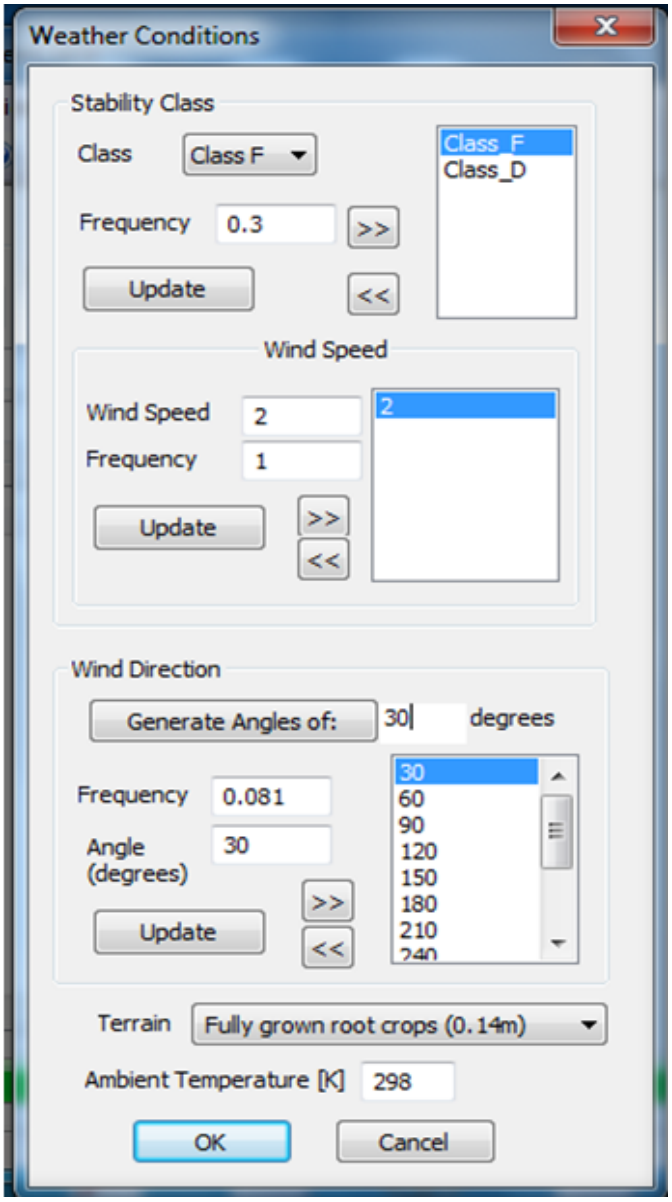

Figure 12. Weather conditions window.

The number of sectors of the wind is defined by the user. The number of sectors can be generated automatically by specifying the angle of the sector. The user then can highlight each sector and enter the probability of each wind direction for all the stability classes and wind speeds defined earlier. Again, the user will need to click on the arrows >> in order to add the values for the wind direction or << in order to delete them. It is up to the user to make sure that the sum of all the probabilities for each parameter equals 1.0.

Table 5. Surface roughness coefficient, z_0 [6].

Terrain classification	Terrain description	Surface roughness, z_0, meters
Highly urban	Centers of cities with tall buildings, very hilly or mountainous area	3-10
Urban area	Centers of towns, villages, fairly level wooded country	1-3
Residential area	Area with dense but low buildings, wooded area, industrial site without large obstacles	1
Large refineries	Distillation columns and other tall equipment pieces	1
Small refineries	Smaller equipment, over a smaller area	0.5
Cultivated land	Open area with great overgrowth, scattered houses	0.3
Flat land	Few trees, long grass, fairly level grass plains	0.1
Open water	Large expanses of water, desert flats	0.001
Sea	Calm open sea, snow covered flat, rolling land	0.0001

At the bottom of the dialog box, the user can define the surface roughness from the drop-down list. The surface roughness is used for the dispersion model as discussed in the

SLAB model section. Obstacles on the ground over which the plume is dispersing will have a tendency to break up the plume. This effect is quantified in the gas dispersion models by a surface roughness coefficient. Typical surface roughness lengths, as used in many models, are given in the Table 5.

Leak locations

The total inventory of the module is assumed to be infinite. This infinite inventory is available for release from any equipment specified in the module in case of leak. The release and frequency characteristics of the equipment defined by a module are approximately modeled by uniformly distributing 'virtual' leak sources over the module plan area. Each of these sources can leak the inventory as specified. Hence the sources are assumed to be interconnected, i.e., a leak in any equipment in the process module can be fed from the whole module infinite inventory.

The user can define as many leak locations as possible. This is done by the user specifying the number of elements in the x and y directions as shown in the main window in Figure 13. The number of elements specified as equally distributed over the area of the process module and placed on grid points, as shown in Figure 13. The program then allocates each leak source at the center of the element. If the number of elements is set to 1, then all leaks are modeled as coming from the geometric center of the process module.

It should be noted that the larger the number of a defined leak sources, the lower the probability of a leak at each source, and hence the lower the probability of damage which underestimates the risk. Therefore, the user can define the optimum number of leaks which should be based on the size of the module. A rule of thumb is that the process module can be divided into a number of elements such that the size of each element is between 1 m^2 to 4 m^2 taking into consideration the number of elements.

.

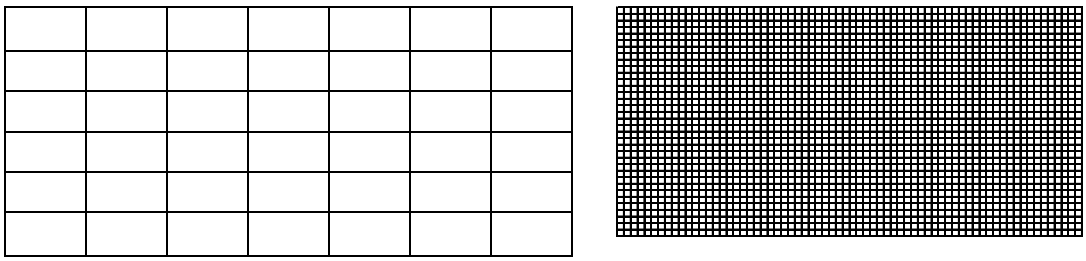

Small Number of elements means few leak locations (7x6).

Increasing the number of elements increases the number of locations (68x34).

Figure 13. Examples showing different user-defined number of elements in a module.

Frequency Analysis

The risk is always a function of frequency and consequence. When screening to find the most likely scenarios to cause harm or escalation at a point, the risk is the likelihood of a particular defined event, defined by a frequency. Frequencies are always presented on an annualized basis (per year) and on a unitized basis (per year per kilometer of pipe, for instance). Sometimes the risk is a frequency resulting from a base frequency multiplied by one or more conditional probabilities. The likelihood of having a cloud fire at a point

is the likelihood of leak scenarios, which ignite. Each leak scenario will search for ignition sources to calculate ignition probability. Probabilities have no units and a value between 0 and 1.

Using the Monte Carlo simulation, the program generates thousands of scenarios based on the user-defined number of hole sizes, leak locations, weather conditions and so on. The frequency of each scenario resulting in explosion can be calculated using equation 22.

$$F_i = f_t \times P_{LS} \times P_{LL} \times P_{WD} \times P_{WS} \times P_{SC} \times P_{ig} \quad (22)$$

where

F_i is the frequency of explosion,

f_M is the frequency of leak in the module,

P_{LS} is the probability of leak size,

P_{LL} is the probability of the leak location,

P_{WD} is probability of the wind direction,

P_{WS} is probability of the wind speed,

P_{SC} is probability of the stability class, and

P_{ig} is probability of the ignition.

The frequency of leak in a module, f_t , is calculated by summing all the frequencies for each type of equipment using the following equation:

$$f_t = \Sigma N_k f_k \quad (23)$$

Where

N_k is the number of equipment of type k,

f_k is the frequency of leak for equipment k.

The probability of leak locations, P_{LS}, is calculated based on the number of leak locations which are specified by the user. As discussed in the previous sections, the user can define the number of elements in the x and y directions to represent the leak locations. The number of leak locations, N_S, is calculated using the following equation:

N_S = (No. of elements in x-direction) * (No. of elements in y-direction) (24)

and hence,

$$P_{LS} = 1/N_S \quad (25)$$

The probability of ignition, P_{ig}, is calculated using equation 17, which is based on the release mass flow rate. The probabilities of leak size, wind speed, wind direction and stability class are defined by the user.

Consequence Analysis

The program has been embedded with the models required to perform an explosion consequence analysis. These models include the flow of gas through a hole source model, SLAB dispersion model, and Multi-energy explosion model. The details of each of these models have been discussed in Chapters II and III. This section describes how each model is carried out within the program.

Flow of gas through a hole model

As pointed out earlier, most of the gas leaks from process plant will initially be sonic, or choked [10]. Therefore, the program will always assume a chocked flow and hence, uses equations 3 and 4 to calculate the release velocity and mass flow rate, respectively. The user defines the fuel type, the source pressure (psig) and temperature (^{o}K), and the release hole size (m). The program evaluates the fuel type and accordingly, selects the appropriate heat capacity ratio and molecular weight. The hole release size is used to calculate the area of the hole. After that, the program calculates the mass flow rate in (kg/s) and uses it in equation 17 to calculate the ignition probability, P_{ig}. In addition, the program calculates the release velocity (m/s) and feeds it to the SLAB model to calculate the volume of the gas cloud.

SLAB model

The program uses the SLAB model to calculate the volume of the gas cloud. The release velocity obtained from the source model is fed into the SLAB model as well as the user

defined values for the stability class and wind speed. The volume of the gas cloud is calculated based on its shape. In this case, the cloud shape is defined by the SLAB model, which describes the changes in width and height. An approximate representation of the cloud shape is shown in Figure 14. A practical method has been applied to determine the height and width of each cloud section at a specific downwind distance interval, represented by D, throughout its travelling distance.

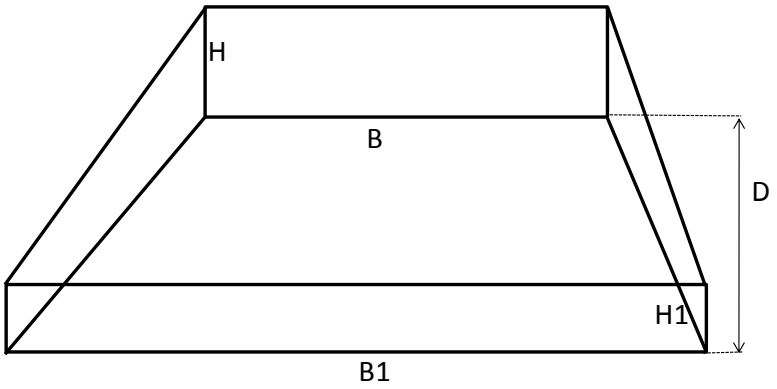

Figure 14. Representation of volume in the cloud using SLAB model.

Each cloud cross-section has two heights H and H_1 and two widths B and B_1. Basically, *D* represents the value of the integration step in the Runge-Kutta method which is used to integrate the differential equations in the SLAB model. At each integration step, the volume of each cloud section can be calculated using equation 26.

$$V = \frac{D}{3}\left(H_1 B_1 + HB + \frac{1}{2}\left(H_1 B + HB_1 \right) \right) \tag{26}$$

At the end of the integration process, the total cloud volume is the sum of all cloud sections. The program only considers the cloud volume inside the congested module that contributes to the blast damage. The other portions of the cloud that are outside the module are not considered in the explosion calculations. A procedure that is used by the program to estimate the gas cloud in the congested module is as follows:

- Calculate the volume of the gas cloud up to the Lower flammability limit (LFL) of the selected fuel type. The program also computes the distance to the LFL point.
- If the LFL point is found to be located outside the module, then the program calculates the distance from the release point to the edge of the module at the projected wind direction.
- The program then recalculates the cloud volume based on the computed distance from the release point to the edge of the module.

In case that the cloud volume is larger than the module volume, then the module volume will be used instead in the explosion model calculations. In addition, if the height of the cloud exceeds the height of the module, the program in that case will use the later instead for computing the cloud volume.

The program calculates the distance from the release point to the edge of the module using trigonometric functions. Once a release point is defined by the program, the

program determines the x and y coordinates of the release point inside the module with respect to the center of the module (0,0), as shown in Figure 15.

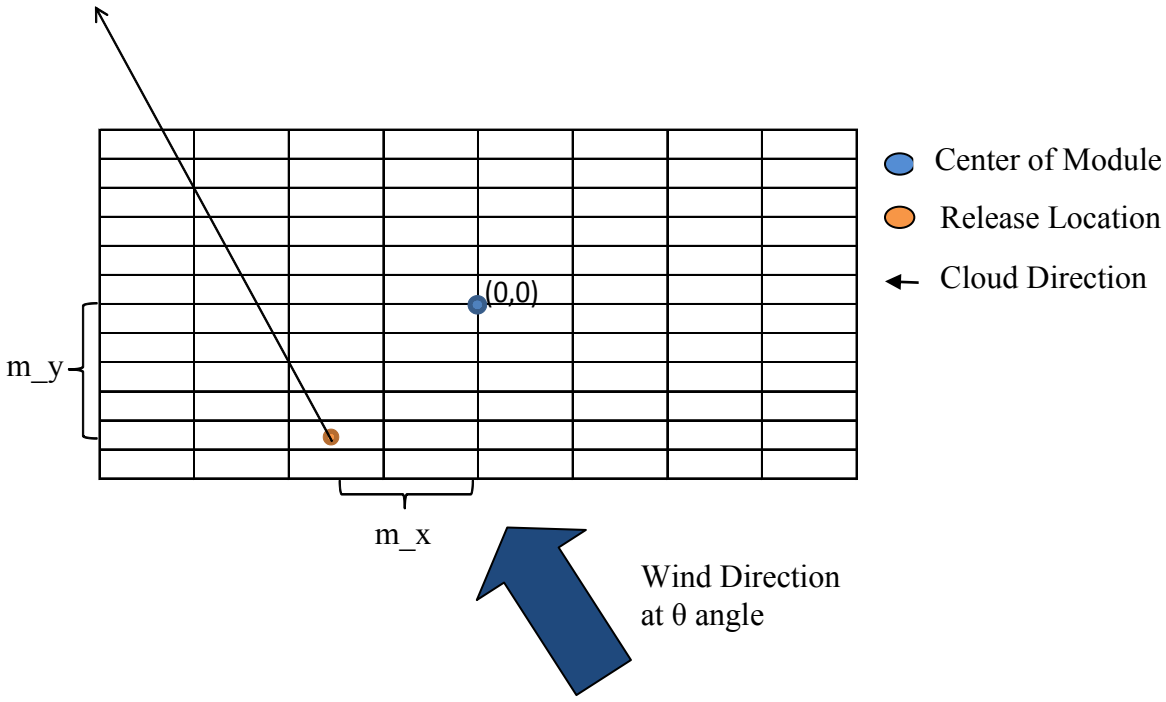

Figure 15. Representation of release source location inside the module as well as the wind direction.

In order to calculate the distance to the edge of the module, the wind direction where the cloud is projected, is used. The program defines β as the angle of the line from the leak point to the corner of the module. The corner angle is important in order to select the appropriate trigonometric function to calculate the distance to the edge of the module at a specific wind direction.

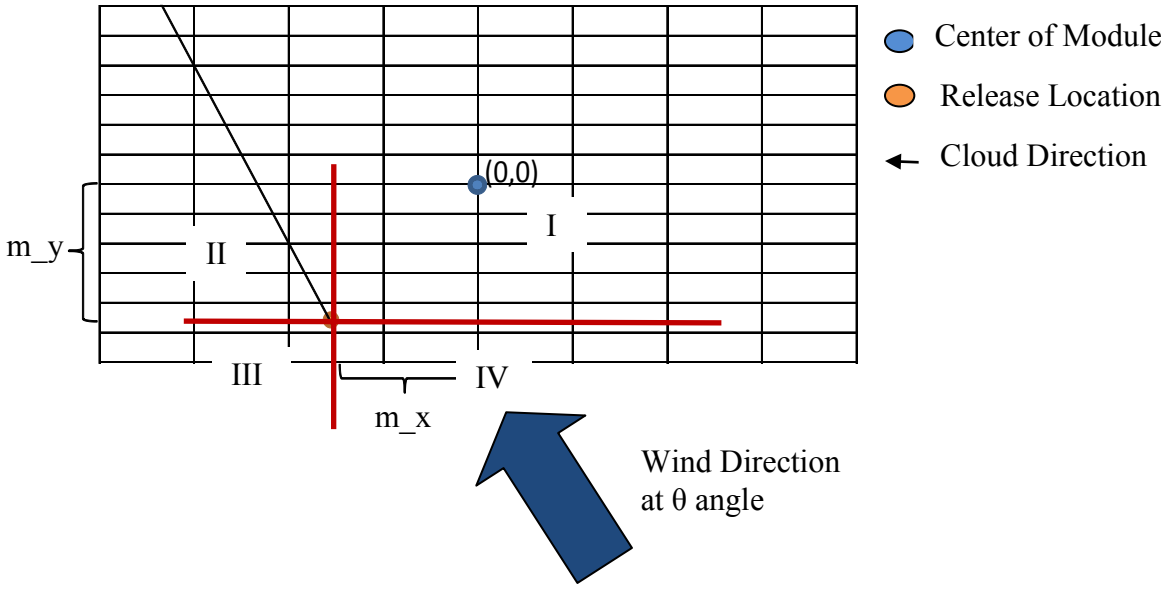

Figure 16. An illustration of the four quadrants used to compute the distance from the release point to the edge of the module.

The program divides the module to four quadrants based on the location of the release source, as shown in Figure 16. The following equations are used to calculate the distance from the release source to the edge of the module in each quadrant:

Quadrant I (0<θ<90 and 0<β<90)

$$\text{If } \theta < \beta\text{: } DLM_x = \frac{Lx}{2} - m\_x\,,\ DLM = \frac{DLM_X}{\cos\theta}$$

$$\text{If } \theta > \beta\text{: } DLM_y = \frac{Ly}{2} - m\_y\ \ DLM = \frac{DLM_Y}{\sin\theta}$$

Quadrant II (90<θ<180 and 90<β<180)

If θ<β: $DLM_y = \frac{Ly}{2} - m\_y,\ DLM = -\frac{DLM_Y}{\cos\theta}$

If θ>β: $DLM_x = \frac{Lx}{2} + m\_x\ \ DLM = \frac{DLM_X}{\sin\theta}$

Quadrant III (180<θ<270 and 180< β <270)

If θ<β: $DLM_x = \frac{Lx}{2} + m\_x\ \ DLM = -\frac{DLM_X}{\sin\theta}$

If θ>β: $DLM_y = \frac{Ly}{2} + m\_y,\ DLM = -\frac{DLM_Y}{\cos\theta}$

Quadrant IV (270<θ<360 and 270< β <360)

If θ<β: $DLM_y = \frac{Ly}{2} + m\_y,\ DLM = \frac{DLM_Y}{\cos\theta}$

If θ>β: $DLM_x = \frac{Lx}{2} - m\_x\ \ DLM = -\frac{DLM_X}{\sin\theta}$

where

Lx is the length of the module in the x-direction

Ly is the length of the module in the y-direction

m_x is the x-coordinate of the release point

m_y is the y-coordinate of the release point

DLM is the distance from the release point to the edge of the module

θ is the angle of the wind direction

β is the angle of the line from the release point to the corner of the module

The quadrant is selected by the program based on the angle of the selected wind direction. Once the distance from the release point to the edge of the module is calculated, the cloud volume can be computed over that distance. In addition, the program calculates the coordinates (x_{center} and y_{center}) of the center of the cloud in each quadrant as follows:

Quadrant I

$x_{center} = (0.5*DLM) \cos(\theta)$

$y_{center} = (0.5*DLM) \sin(\theta)$

Quadrant II

$x_{center} = (0.5*DLM) \cos(\theta-90)$

$y_{center} = (0.5*DLM) \sin(\theta-90)$

Quadrant III

$x_{center} = (0.5*DLM) \cos(\theta-180)$

$y_{center} = (0.5*DLM) \sin(\theta-180)$

Quadrant IV

$x_{center} = (0.5*DLM) \cos(\theta-270)$

$y_{center} = (0.5*DLM) \sin(\theta-270)$

TNO multi-energy model

Last step in the consequence analysis process is determining the side-on overpressure through the use of the TNO multi-energy model. Details of the model have been described in Chapter III. Two parameters are required to be fed to the model in order to calculate the overpressure. First, the cloud volume within the congested area, which has already been calculated by the SLAB model, should be fed into the model. Second, is the distance between the center of the cloud and the receptor, i.e., building, which is calculated using an Euclidean equation, as follows:

$$Dist = \sqrt{(x_{center} - x_{Building})^2 + (y_{center} - y_{Building})^2} \quad (28)$$

Where Dist is the computed Euclidean distance, x_{center} and y_{center}, are the coordinates of the center of the cloud and $x_{Building}$ and $y_{Building}$ are the coordinates of the location of the building. The program always assumes a blast strength of 7 which is typical for hydrocarbon processing facilities.

Monte Carlo Simulation

When the relationship between the input parameters and output values is complex and it may not be possible to analytically perform such calculations, the Monte Carlo technique is used. Monte Carlo is a computational technique used to approximate the probability of certain output by running hundreds or thousands of trials using randomly generated

numbers. During a Monte Carlo simulation, the value of each input parameter is sampled randomly from its associated probability distributions. For each set of samples, called an *iteration,* the outcome derived from that sample is documented. The distribution of values of that output from the many iterations, is an estimation of its probability distribution.

The proposed program assigns a discrete cumulative distribution to each input parameter such as the hole size, wind direction, wind speed and stability class based on the user-defined probabilities for each variable. The program also assigns a discrete uniform distribution to the leak location since the leak is equally spread over the module. The program is run N times based on the number of iterations chosen by the user. For each run, a random number is generated, matched to the cumulative distribution of each input parameter and a value of each input parameter is selected accordingly.

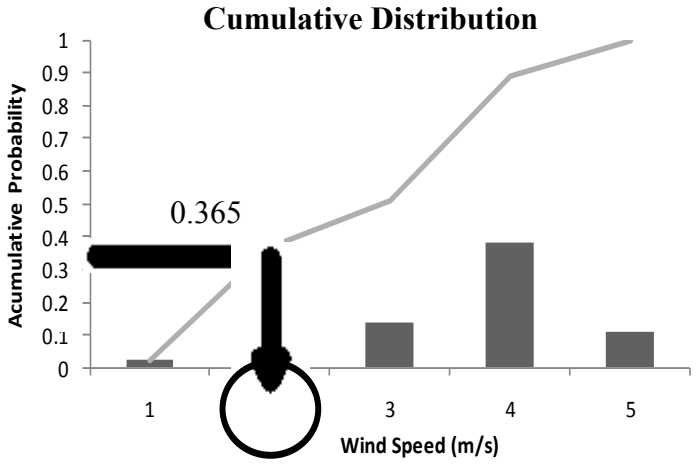

Figure 17. MC simulation of wind speed with 0.365 as random number generated.

Figure 17 shows an example of randomly selecting a value for the wind speed from its cumulative distribution. Using Monte Carlo requires a considerable number of iterations in order to reduce uncertainty in the simulation. The number of iterations that is necessary to produce good data for the output value is not easy to estimate. The quickest technique to determine the necessary number of iterations is to repeat the simulations. The consistency between the results in the two runs of computations can provide an indication of the agreement of fit of the results to the probability distribution required. In case the number of iterations needs to be altered, it can be assumed that the standard deviation of the computed values is proportional to the square root of the number of iterations [35].

Exceedance Calculations

Once the program determines the values for the overpressure as well as the associated frequencies from all possible scenarios, the program then carries out the exceedance calculations. One practical technique to show the results from quantitative risk assessment is through frequency of exceedance curves, or so-called Farmer's curves [38]. When using this method, the consequences are plotted against the complementary cumulative distribution of the frequencies. Table 6 shows how to obtain the complementary cumulative frequencies. Basically, the program starts by sorting the frequencies in decreasing order and consequences in ascending order. Then, the frequency of exceedance, F'_i, for each scenario or consequence, s_i or C_i, can be calculated by summing the frequencies associated with scenarios or consequences of

higher magnitudes. Thus, the calculation of cumulative frequency, *F'*i, for *C*>*C*i should answer the question of what the total frequency of events with C >*C*i (or in other words, frequency of exceeding Ci).

Table 6. Scenarios showing how to obtain cumulative frequency (reproduced) [38].

Scenario	Frequency (Descending order)	Consequence (Ascending order)	Complementary Cumulative Frequency (Descending order)
s_1	f_1	C_1	$F_1' = f_N + f_{N-1} + \ldots + f_1$
s_2	f_2	C_2	⋮
s_3	f_3	C_3	⋮
⋮	⋮	⋮	⋮
s_{N-1}	f_{N-1}	C_{N-1}	$F'_{N-1} = f_N + f_{N-1}$
s_N	f_N	C_N	$F'_N = f_N$

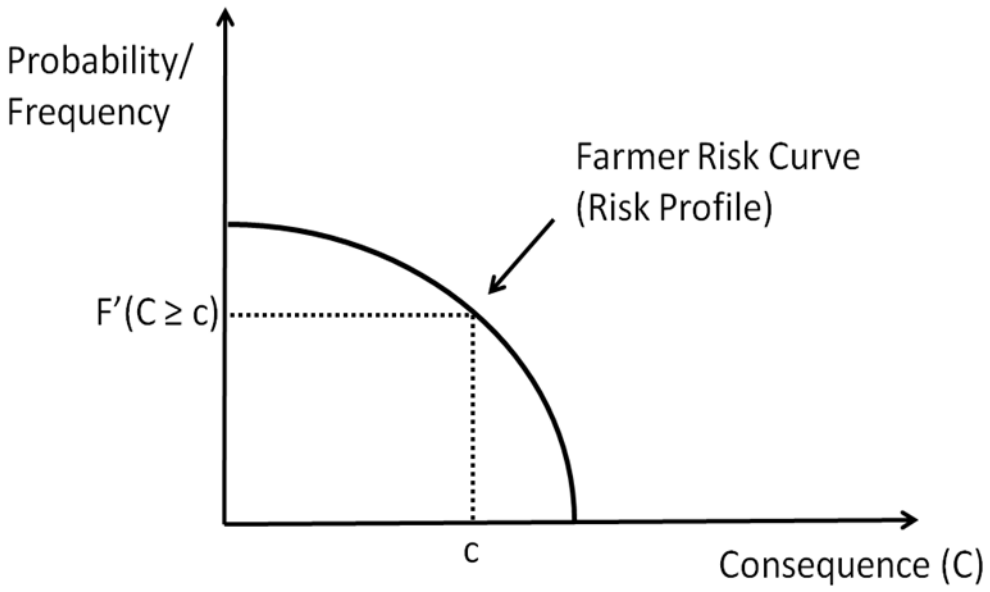

Figure 18. An example of a Farmer curve (Redrawn) [38].

The program prints out the values of the overpressure as well as the associated frequency of exceedance in a tabulated format. Excel can then be used to plot the exceedance curve (Figure 18).

There are different approaches to make use of overpressure exceedance curves. One approach is to base design loads on a probabilistic argument. In this way, a probabilistic acceptance criterion must be developed and accepted. An example could be that the probability of a building receiving an overpressure of 1 psi and, hence suffering undesirable damage shall be less than 10^{-4}/year. A different way is to evaluate how efficient are the mitigation measures. This can be done by comparing the exceedance

results calculated using the base scenarios with scenarios pertinent to the mitigation measure under assessment (e.g., deluge system).

CHAPTER V

CASE STUDY

This chapter presents a case study to demonstrate the application of the proposed program discussed in the preceding chapters. The case study is a debutanizer process.

Case Description

Process overview

A debutanizer is used to remove dissolved light hydrocarbon components through C4 (butane). The debutanizer column operates at about 255 psig. The amount of butane in the column bottoms is determined by controlling the debutanizer tray temperatures. A process flow diagram is given in Figure 19. There are two feeds with different hydrocarbon compositions which enter the debutanizer at different tray elevations. The butane in the bottoms stream is concentrated in the lightest liquid product stream: light naphtha. The stripping vapors flow up through the lower portion of the debutanizer. The reboiler pumps pump the bottoms material from the column bottom to the reboiler. The debutanizer overhead vapors leave the column to the air-cooled, fin-tube condensers, which condense the overheads to 130°F. From overhead condensers, the effluent separates into vapor and liquid phases in the debutanizer overhead receiver. Debutanizer off-gas leaves on pressure control by regulating the column pressure. The off-gas flows to a gas recovery plant. The hydrocarbon liquid from the debutanizer receiver is pumped by the debutanizer reflux pumps. Part of the stream goes back to the debutanizer column

as a controlled reflux. This reflux regulates the temperature at tray 23 and governs the butane split between the column overheads and the bottoms stream. The stabilized C5+ (pentane and heavier hydrocarbons) debutanizer bottoms material is pressured from the bottom of the column on level control to the downstream fractionation plant.

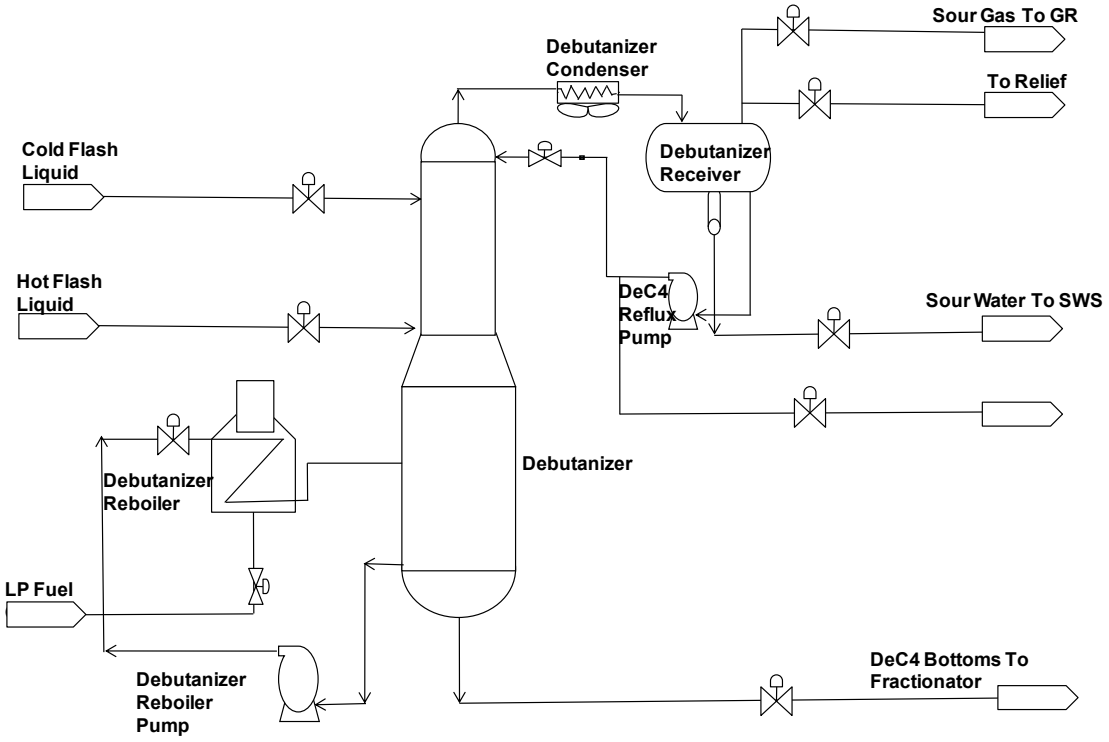

Figure 19. A process flow diagram of the debutanizer process.

Plant layout

The plant site layout is presented in Figure 20. The in-plant building is located about 85 meters to the north-west of the Debutanizer unit. The study goal is to estimate the risk to the building from the Debutanizer unit from side-one overpressure perspective.

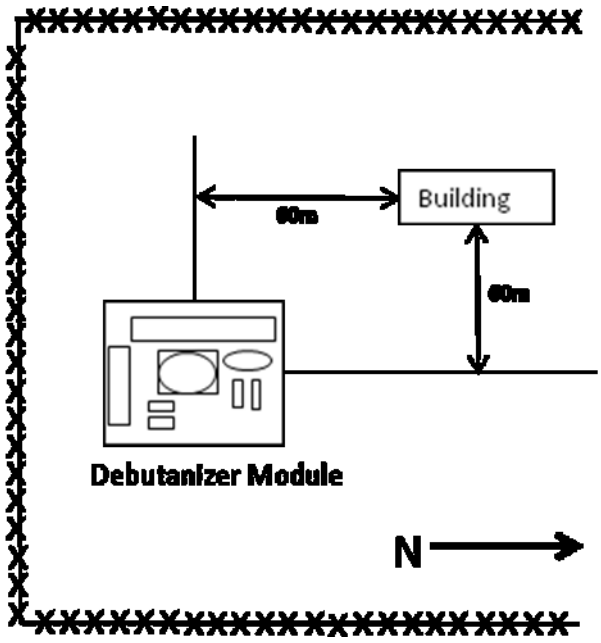

Figure 20. The plant layout.

Weather conditions

Figure 21 shows the wind rose used in this case, which gives the probabilities of wind direction at each wind speed.

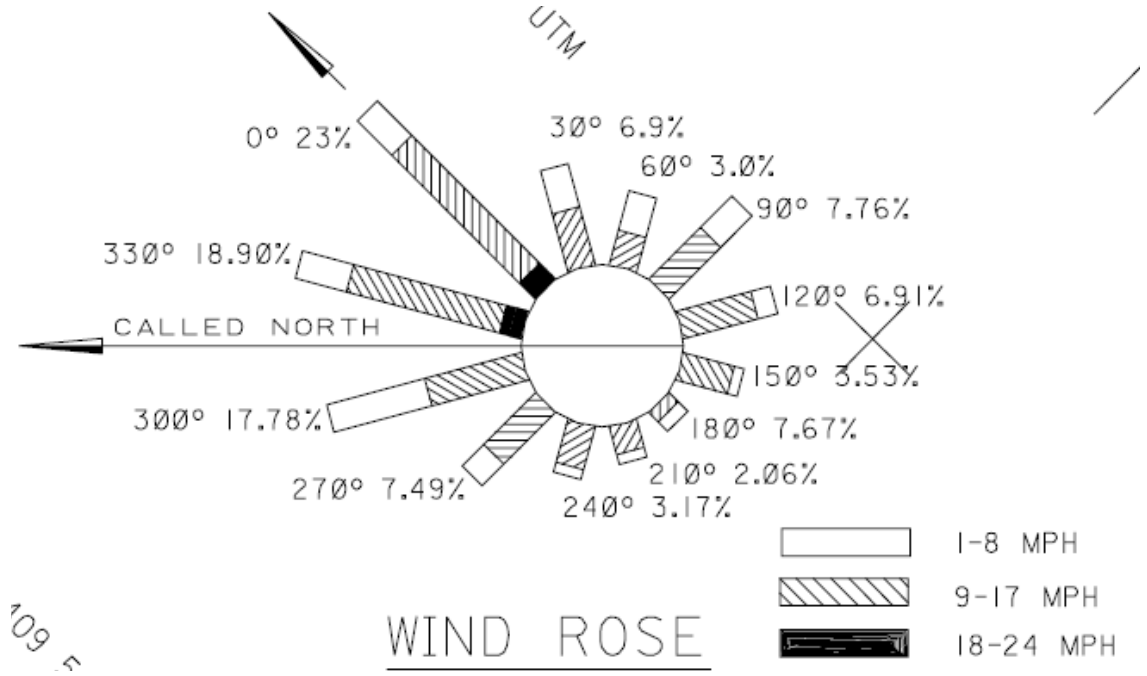

Figure 21. The wind rose for the case study.

Taking measurements from the wind rose, the wind distribution for 3 wind speeds has been calculated. The results are presented in Table 7.

Table 7. Wind distribution (in mm).

Wind Speed Range (mph)		0	30	60	90	120	150	180	210	240	270	300	330
1	8	7	6	5	6	3	1.5	2	1.5	1	4.5	15	8
9	17	26	10	5	10	11	7.5	2	4	6	10.5	14.5	23
18	24	3	0	0	0	0	0.0	0	0	0	0	0	3

Table 8 presents the percentage wind direction distribution over 3 representative wind speeds. This has been calculated using a scaling factor to normalize the results. The representative wind speeds are simply the mean average of the wind speed range.

Table 8. Wind distributions in percentages.

Avg. Wind Speed (m/s)	0	30	60	90	120	150	180	210	240	270	300	330
2.0	0.04	0.03	0.03	0.03	0.02	0.01	0.01	0.01	0.01	0.02	0.08	0.04
5.8	0.14	0.05	0.03	0.05	0.06	0.04	0.01	0.02	0.03	0.05	0.07	0.12
9.4	0.02	0	0	0	0	0	0	0	0	0	0	0.02

Typical wind speeds selected for dispersion modeling will be 5m/s for weather stability D and 2m/s for weather stability F. Weather stability F and D are split 30%:70%, respectively.

Modeling parameters

Table 9 shows the modeling parameters which will be used by the program in addition to the atmospheric conditions described in the previous section.

Table 9. Modeling parameters.

<table>
<tr><th>Modeling Parameter</th><th>Description</th></tr>
<tr><td>Equipment Count</td><td>
<table>
<tr><th>Equipment</th><th>Count</th><th>Leak Frequency (1/yr) [23]</th></tr>
<tr><td>Vessel</td><td>2</td><td>1.50E-04</td></tr>
<tr><td>Pumps</td><td>2</td><td>1.71E-02</td></tr>
<tr><td>Heat Exchanger</td><td>2</td><td>1.50E-04</td></tr>
<tr><td>Pipework</td><td>450</td><td>3.60E-05</td></tr>
<tr><td>Flanges</td><td>214</td><td>8.80E-06</td></tr>
<tr><td>Valves</td><td>78</td><td>2.30E-04</td></tr>
<tr><td>Fittings</td><td>144</td><td>4.70E-04</td></tr>
</table>
</td></tr>
<tr><td>Operating Conditions</td><td>Pressure = 225 psig
Temperature = 400 ^{o}K</td></tr>
<tr><td>Equivalent Fuel</td><td>Butane</td></tr>
<tr><td>Hole Size Distribution</td><td>
<table>
<tr><th>Hole Size (mm)</th><th>Probability [37]</th></tr>
<tr><td>10</td><td>0.45</td></tr>
<tr><td>20</td><td>0.20</td></tr>
<tr><td>50</td><td>0.15</td></tr>
<tr><td>100</td><td>0.10</td></tr>
<tr><td>150</td><td>0.05</td></tr>
<tr><td>200</td><td>0.03</td></tr>
<tr><td>Full Bore (12")</td><td>0.02</td></tr>
</table>
</td></tr>
<tr><td>Ambient Temperature</td><td>300 ^{o}K</td></tr>
<tr><td>Surface Roughness</td><td>0.1 m</td></tr>
<tr><td>Module Size</td><td>Length (x) = 40 meters
Width (y) = 30 meters
Height (z) = 20 meters</td></tr>
<tr><td>Distance from Module to Building</td><td>56 meters (x=40, y=40)</td></tr>
<tr><td>No. of Leak Locations</td><td>100 (No of elements 10 x 10)</td></tr>
</table>

Results and Discussion

The side-on overpressure exceedance curve for the case study was calculated by the program and plotted in Microsoft Excel, as shown in Figure 22.

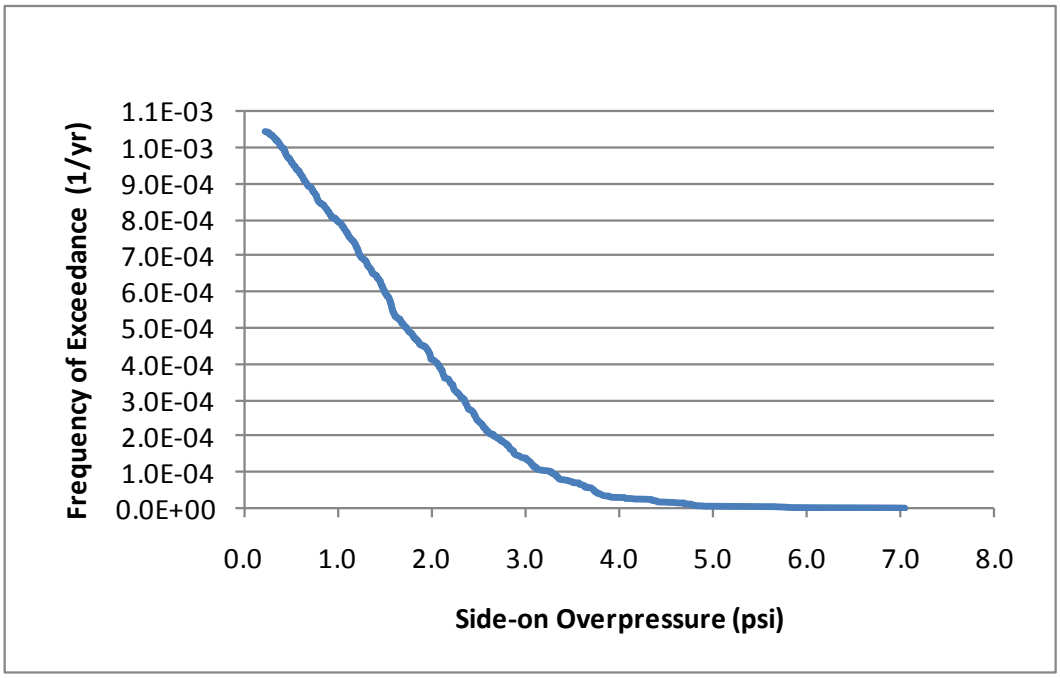

Figure 22. The side-on overpressure exceedance curve at 56 meters distance.

Figure 22 illustrates that the frequency of a large overpressure as a result of an explosion decreases as the overpressure and the severity of the explosion increases. This implies that most probably the overpressure would be fairly small if an explosion had occurred.

The overpressure exceedance curve in this case study is used to estimate if the frequency of the building receiving a certain overpressure for which the building is designed to

withstand, can be accepted and if the overpressure is not acceptable, relocation or redesign of the building, or other measures must be considered. For example, the building in this case study is designed to withstand a pressure of 1 psi, which means that this pressure or a higher pressure occurs once every 1,250 years because the frequency is 8×10^{-4}. If this frequency can be accepted, then the design pressure is correct. However, if this frequency cannot be accepted, then one option is to strengthen the design of the building in order to withstand the overpressure associated with the acceptable frequency. For example, if the acceptable criteria or frequency of explosion is one every 10,000 years ($1x10^{-4}$), then according to Figure 22, the building must be designed to survive an overpressure of 3.3 psi. It is of course possible to experience a higher pressure, e.g., 5 psi but the frequency of such a pressure is about 6×10^{-6}.

Other available alternatives would be to relocate the building further away from the process unit. Figure 23 shows different exceedance curves calculated at different building locations for the same case study. In this case, the building should be located at about 140 meters from the center of the process unit to ensure that the frequency of exceeding 1 psi is once every 10,000 years.

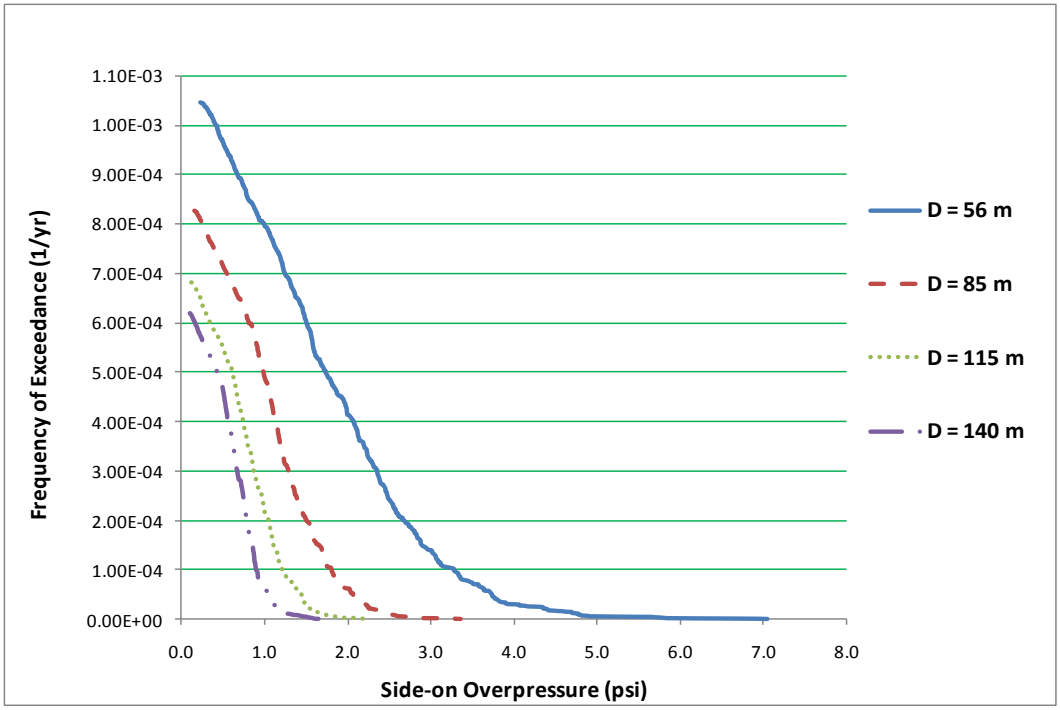

Figure 23. The side-on overpressure exceedance curve at different distances.

The program can also be used to investigate different aspects of vapor cloud explosion. One example would be to relate the calculated overpressure to the gas cloud size since the volume of the gas cloud is assumed to be at stoichiometric concentration. The calculated overpressure increases with the gas cloud size in the congested area as shown in Figure 24. It can be shown from the figure that the calculated overpressure in a congested area can be often lower than the maximum overpressure due to the fact that the gas cloud size might be small. In addition, the percentage of the cloud volume filling the module volume is below 20% and always depends on the probability distribution of the leak size, wind direction, and leak location. The highest filling percentage possible at

a specific leak size would be if the leak location is at the corner of the module and the wind direction is blowing towards the module.

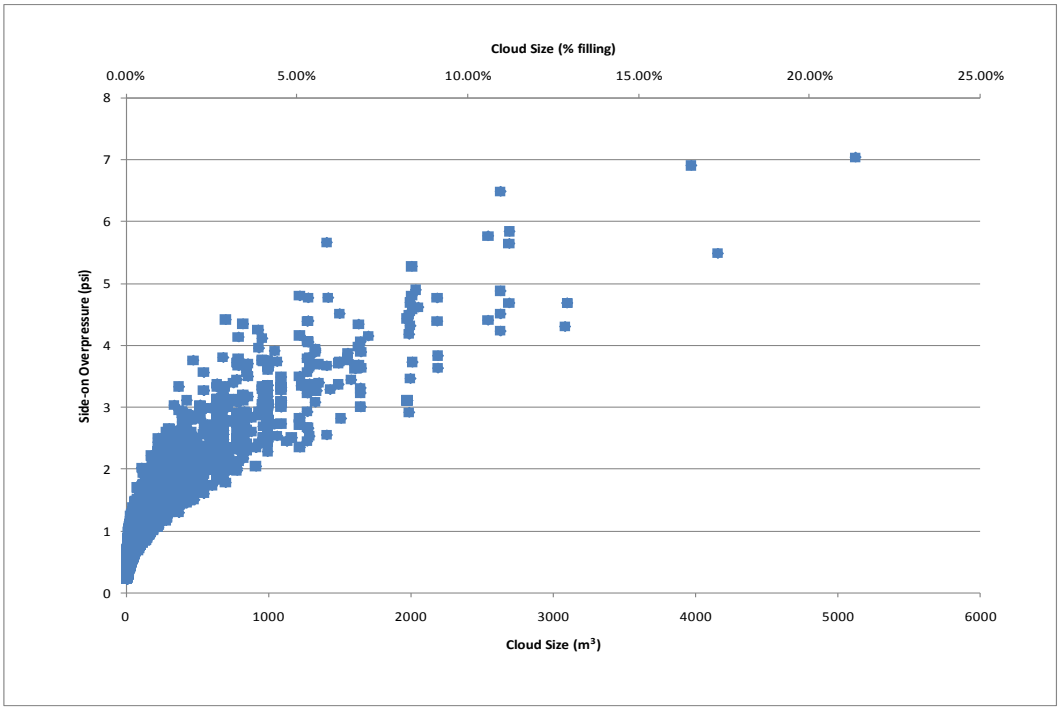

Figure 24. Cloud size vs. overpressure.

Another example would be to examine the impact of the number of virtual leak locations in the overall risk estimation. Figure 25 illustrates the result of increasing or decreasing the number of leak locations in a quantitative risk study. For instance, if the building in the case study can survive an overpressure of 1 psi, then selecting fewer leak locations will result in higher frequency of exceedance, while choosing a large number of leak locations results in lower frequencies. Therefore, selecting the number of leak location is important in analyzing risk. It should be noted that the smaller the number of leak

locations, the larger the area per each leak location which would increase the uncertainty of the size of the cloud and therefore, the uncertainty of the resulting overpressure.

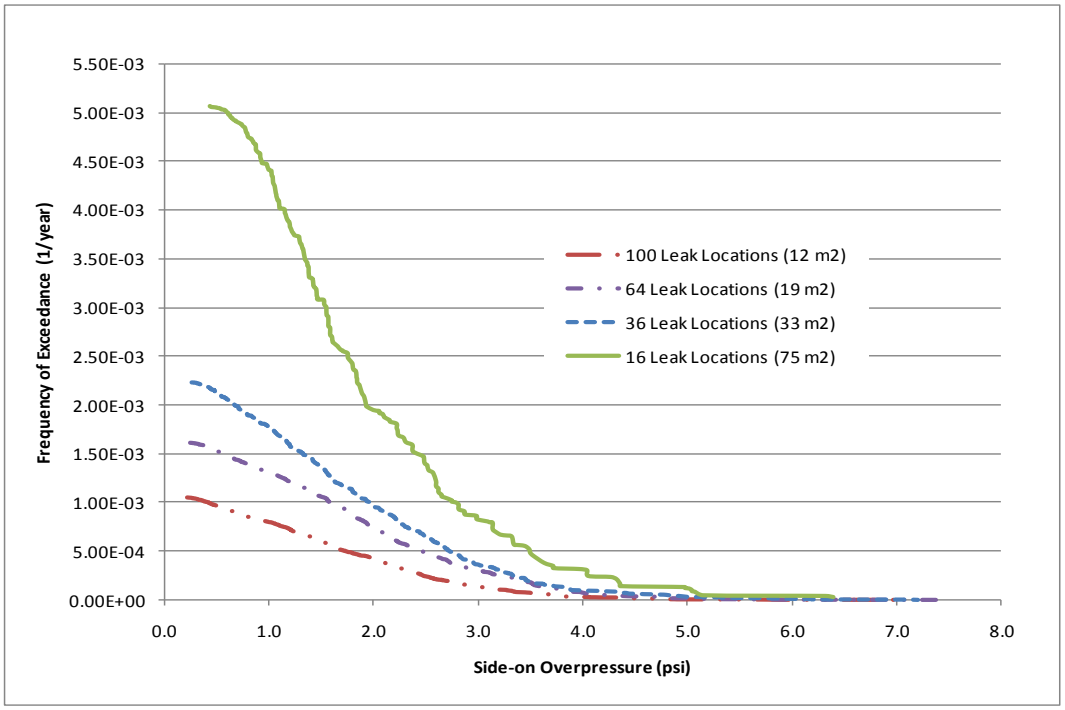

Figure 25. Impact of number of leak locations on the overall risk.

One of the main advantages of the program is the Monte Carlo technique, which allows the user to decide the level of resolution in terms of how many groups the different variables, such as hole sizes, are to be divided into. When selecting a high resolution, a better accuracy is achieved. In a conventional worksheet technique, the number of groups is limited (usually 3 groups).

Improved accuracy of the analysis has been achieved in the proposed program because of its ability to use as many categories as needed. Figure 26 shows how much the results can be influenced. This is demonstrated by running the program with 3 and 7 categories of hole sizes.

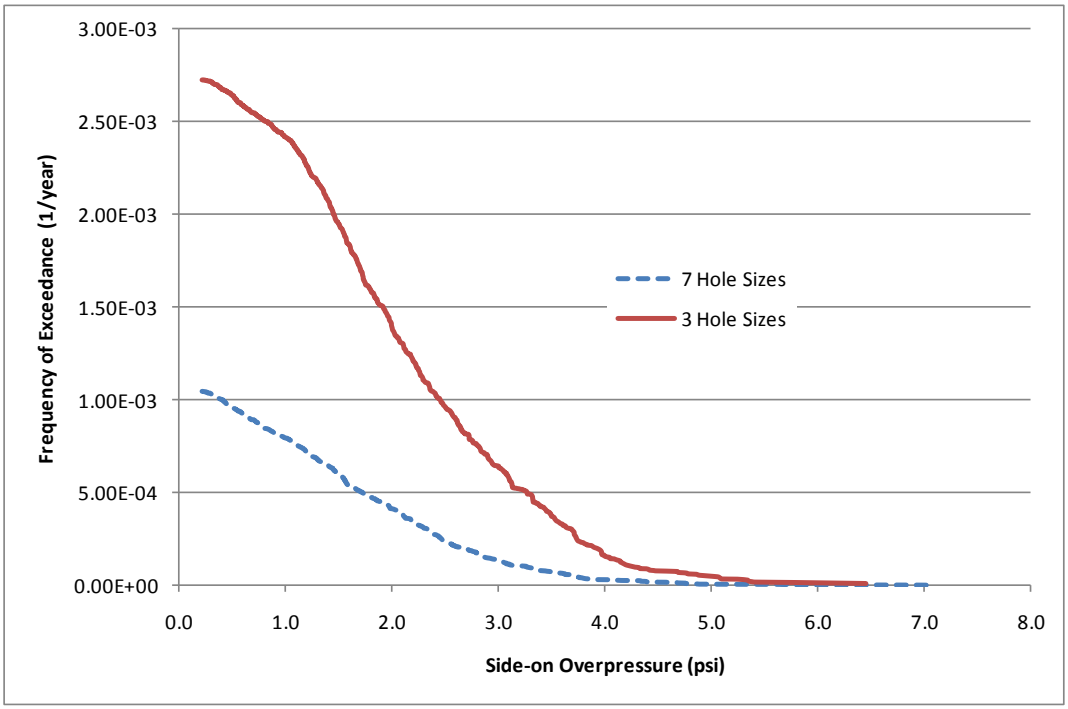

Figure 26. Overpressure exceedance curve using different numbers of categories.

Results Validation

The overpressure results obtained by this model were compared to the overpressure values obtained from two public domain programs using the same case study. The two programs are PHAST by Det Norske Veritas (DNV) [39], and CANARY by Quest

Consultant Inc. [40]. These two programs are specialized in fire and explosion consequence modeling as well as toxic releases.

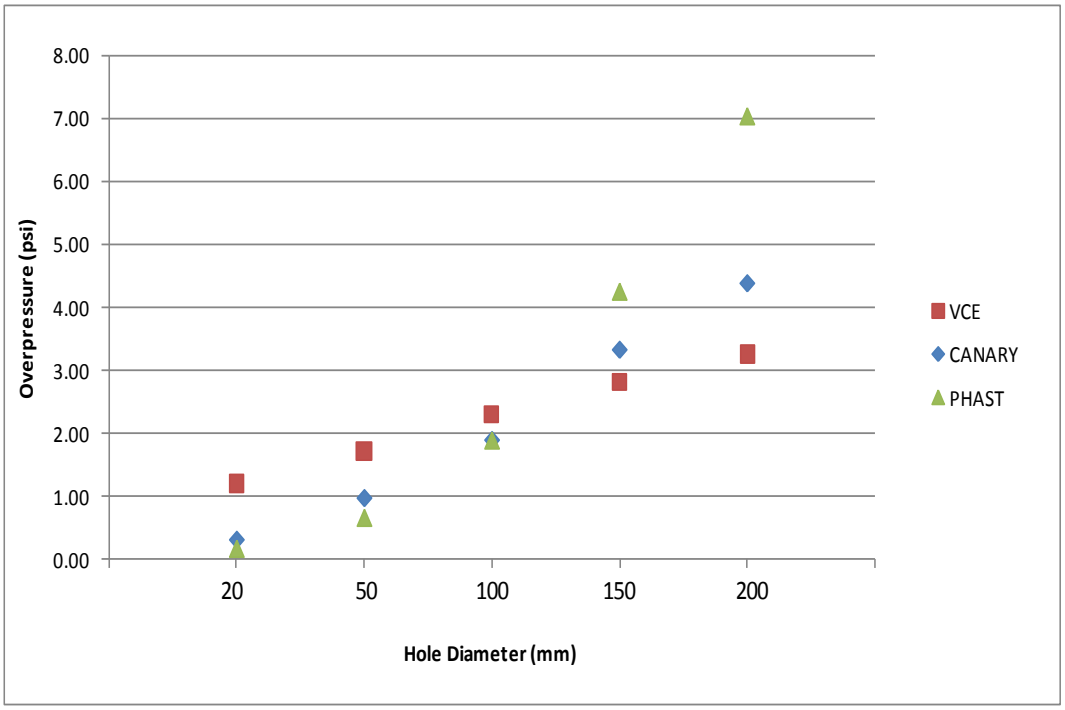

Figure 27. Comparison of explosion overpressure results obtained from two different programs with the results using the proposed program.

Figure 27 shows the overpressure plotted against the hole diameter for the three programs while keeping the other parameters unchanged. In comparison with the other two programs, the proposed program (VCE) over predicts the overpressure at lower hole diameters and under predicts the overpressure at higher hole diameters. The different results are attributed to the differences in modeling assumptions and the modeling tools used in calculating the overpressures. Although this comparison simply tests the

explosion overpressure, the result is encouraging and is within the uncertainty bounds (a factor of 2) usually related to risk analysis.

CHAPTER VI

CONCLUSIONS AND FUTURE WORK

Conclusions

The main advantage of using the exceedance technique to estimate the explosion overpressure is its ability to investigate the risk distribution from all possible explosion scenarios. This includes the many thousand possible dispersion scenarios estimated by SLAB with ignition probabilities to produce a collection of possible explosion scenarios, using Monte Carlo techniques. The results can be expressed as the frequency of exceeding a given overpressure at a specific location, including occupied buildings on a hydrocarbon processing site. Empirical models, such as the Multi-energy explosion method, are used due to their speed of computation and because of a general lack of 3D information on plant layouts in the early design phases of a project. In some cases though, a full CFD approach should be used if the safety risk information is deemed critical to the site.

Future Work

The future works in this research include conducting additional validations of the results produced by the program with other available software or published large-scale tests. In addition, future research should consider further analysis of the explosion using additional variables such as ignition location, ignition intensity, fluid composition and time of ignition. Having more variables involved in the analysis will better describe the

characteristic of the explosion that had occurred. Additional models describing the release of liquids, or two-phase can be embedded in the future versions of the program.

LITERATURE CITED

1. F.P. Lees, Loss Prevention in the Process Industries, 3rd ed., Elsevier Butterworth-Heineman, Burlington (MA), 2005.

2. Center for Chemical Process Safety (CCPS), Guidelines for Evaluating Process Plant Buildings for External Explosions and Fires, American Institute of Chemical Engineers, New York, 1996.

3. American Petroleum Institute, Chemical Manufacturers Association, Recommended Practice 752, Management of Hazards Associated with Locations of Process Plant Buildings, API Standard 752, 1st ed., Washington, DC, 1995.

4. W.G. Garrison, Major fires and explosions analysed for 30-year period, Hydrocarbon Processing (1988), 115-118.

5. E.M. Lenoir and J.A. Davenport, A survey of vapor cloud explosions: second update, Process Safety Progress 12 (1993), 12-26.

6. Center for Chemical Process Safety (CCPS), Guidelines for Chemical Process Quantitative Risk Analysis, 2nd edition. American Institute of Chemical Engineers, Center for Chemical Process Safety, New York, 2000.

7. O. Talberg, O.R. Hansen, J.R. Bakke, and K. van Wingerden, "Application of a CFD-based probabilistic risk assessment to a gas-handling plant", International European Safety Management Group (ESMG) Symposium, 2001, 27-29.

8. D. Crowl and J. Louvar, Chemical Process Safety: Fundamentals with Applications, 2nd ed., Prentice Hall PTR, Upper Saddle River (NJ), 2002.

9. Health and Safety Executive (HSE), Offshore Hydrocarbon Release Statistics and Analysis 2002, HID Statistics Report, HSR 2002 002, HSE, Bootle (UK), 2003.

10. Center for Chemical Process Safety (CCPS), Guidelines for Consequence Analysis of Chemical Releases, American Institute of Chemical Engineers, Center for Chemical Process Safety, New York, 1999.

11. O. Zeman, The dynamics and modeling of heavier-than-air, cold gas releases, Atmos. Environ. 16 (1982), 741-751.

12. D.L. Ermak, S.T. Chan, D.J. Morgan, and L.K. Morris, A comparison of dense gas dispersion model simulations with Burro series LNG spill test results, J. Haz. Materials 6 (1982), 129-160.

13. D.L. Ermak, User's Manual for SLAB: An Atmospheric Dispersion Model for Denser-Than-air Releases Manual, Lawrence Livermore National Laboratory, Livermore (CA), 1990.

14. S.C. Chapra and R.P. Canale, Numerical Methods for Engineers, 5th ed., McGraw-Hill, New York, 2006.

15. H. Spencer and P.J. Rew, Ignition Probability of Flammable Gases, HSE Contractor Report WSA/RSU8000/026, HSE Books, London (UK), 1996.

16. J.L. Woodward, Estimating the Flammable Mass of a Vapor Cloud, Center for Chemical Process Safety, American Institute of Chemical Engineers, New York, 1998.

17. P.J. Rew and L. Daycock, Development of a Method for the Determination of On-site Ignition Probabilities, HSE Contractor Report WSA/226, HSE Books, London (UK), 2004.

18. P.J. Rew, H. Spencer, and L. Daycock, Offsite ignition probability of flammable gases, Journal of Hazardous Materials 71 (2000), 409-422.

19. A.W. Cox, F.P. Lees, and M.L. Ang, Classification of Hazardous Locations, Institution of Chemical Engineers, Rugby (UK), 1990.

20. P.J. Rew, H.S. Spencer, A.P. Franks, A Framework for the Ignition Probability of Flammable Gas Clouds, HAZARDS 13, IChemE North Western Branch, Manchester (UK), 1997.

21. E. Dahl, T.I. Bern, M. Golan, and G. Engen, Risk of Oil and Gas Blowout on the Norwegian Continental Shelf, SINTEF, Trondheim (Norway), 1983.

22. T.A. Kletz, Unconfined vapor cloud explosions, Loss Prevention 11 (1977), AICHE.

23. E&P Forum, Hydrocarbon Leak and Ignition Database, EP Forum Report No. 11.4/180, E&P Forum, London, May 1992.

24. GexCon, Gas Explosion Handbook, Website: http://www.gexcon.com., Accessed on 02/03/2011.

25. A.C. Berg, The multi-energy method - A framework for vapor cloud explosion blast prediction, Journal Hazardous Materials 12 (1985), 1-10.

26. Q.A. Baker, C.M. Doolittle, G.A. Fitzgerald, and M. Tang, Recent developments in the Baker-Strehlow VCE analysis methodology, Process Safety Progress 17(4) (1998), 297-301.

27. J.S. Puttock, "Fuel gas explosion guidelines - the congestion assessment method", 2nd European Conference on Major Hazards On- and Off-shore, Manchester (UK), 1995, 24-26.

28. J. S. Puttock, "Improvements in guidelines for prediction of vapour-cloud explosions", International Conference and Workshop on Modeling the Consequences of Accidental Releases of Hazardous Materials, San Francisco (CA), 1999, 7-19.

29. J.S. Puttock, M.R. Yardley, and T.M. Cresswell, Prediction of vapor cloud explosions using the SCOPE model, Journal of Loss Prevention in the Process Industries 13 (2000), 419-430.

30. C.A. Catlin, "CLICHE - A generally applicable and practicable offshore explosion model", IChemE Symposium Series No. 68, Part B, 1990, 245-253.

31. C.J. Lea, and H.S. Ledin, A Review of the State-of-the-art in Gas Explosion Modeling, HSE Report 2002/02, London (UK), 2002.

32. G.A. Fitzgerald, "A comparison of simple vapor cloud explosions prediction methodologies", Second Annual Symposium, Mary Kay O'Connor Process Safety Center, Texas A&M University, College Station (TX), 2001, 126-134.

33. Center for Chemical Process Safety (CCPS), Guidelines for the Evaluation of the Characteristics of Vapor Cloud Explosions, Flash Fires and BLEVES, Centre for Chemical Process Safety, AIChE, New York (USA), 1994.

34. V.J. Clancey, "Diagnostic features of explosion damage", Paper presented at the Sixth International Meetings of Forensic Sciences, Edinburgh (Scotland), 1972.

35. J.S. Puttock, "The use of a combination of explosion models in explicit overpressure exceedance calculations for an offshore platform", Proc. Int. Conf. Major Hazards Offshore - practical implications, London (UK), 2000, 341-354.

36. J. Spouge, New generic leak frequencies for process equipment, Process Safety Progress 24 (4) (2005), 249-257.

37. Health and Safety Executive (HSE), Offshore Hydrocarbon Release Statistics 2001, HID Statistics Report, HSR 2001 002, HSE, Bootle (UK), 2002.

38. M. Modarres, Risk Analysis in Engineering, Taylor & Francis, Philadelphia (PA), 2006.

39. DNV, Website: http://www.dnv.com/Phast.html, Accessed on 04/10/2011.

40. Quest, Website: http://www.questconsult.com/canary.html, Accessed on 04/17/2011.

VITA

Name:	Salem Saad S. Alghamdi
Address:	Kingdom of Saudi Arabia Saudi Aramco Loss Prevention Department Planning and Technical Services Division Technical Support Unit
Email Address:	ghamss1i@gmail.com
Education:	B.S., Chemical Engineering, Colorado School of Mines at Golden, CO, 2001 B.S., Math and Computer Science, Colorado School of Mines at Golden, CO, 2001 M.S., Safety Engineering, Texas A&M University, 2011
Employment:	Loss Prevention Engineer, Saudi Aramco, 2001-present